SIAM Rev.
Vol. 40, No. 3, pp. 579–615, September 1998

005

COLLECTIVE COORDINATES AND LENGTH-SCALE COMPETITION IN SPATIALLY INHOMOGENEOUS SOLITON-BEARING EQUATIONS*

ANGEL SÁNCHEZ† AND A. R. BISHOP‡

Abstract. Perturbed, one-dimensional, integrable (i.e., soliton-bearing) equations arise in many applied contexts when trying to improve the (usually highly idealized) description of problems of interest in terms of the purely integrable equations. In particular, when the assumption of perfect homogeneity is dropped to account for unavoidable impurities or defects, perturbations depending on the spatial coordinate must be added to the original equation. In this review, we use the one-dimensional sine-Gordon (sG) equation perturbed by a spatially periodic term as a generic paradigm to discuss the main perturbative techniques available for the study of this class of problems. To place the work in context, we summarize the approaches developed to date and focus on the collective coordinate approach as one of the most useful tools. We introduce several versions of this perturbative method and relate them to more involved procedures. We analyze in detail the application to the sG equation, but the procedure is very general. To illustrate this other examples of the application of collective coordinates are briefly revisited. In our case study, this approach helps us identify perturbative and nonperturbative regimes, yielding a very simple picture of the former. Beyond perturbative calculations, the same example of the inhomogeneous sG equation allows us to introduce a phenomenon, termed length scale competition, which we show to be a rather general mechanism for the appearance of complex spatiotemporal behavior in perturbed integrable systems, as other instances discussed in the review show. Such nonperturbative results are obtained by means of numerical simulations of the full perturbed problem; numerical linear stability analysis is also used to clarify the origins of the instability originated by this competition. To complement our description of the techniques employed in these studies, computational details of our numerical simulations are also included. Finally, the paper closes with a discussion of the above ideas and a speculative outlook on general questions concerning the interplay of nonlinearity with disorder.

Key words. solitons, spatially dependent perturbations, perturbation theories, nonperturbative results, collective coordinates, length scales, sine-Gordon, nonlinear Schrödinger

AMS subject classifications. 35B27, 35Q53, 35Q55, 35B20

PII. S0036144597317418

1. Introduction.

During the past 40 years or so, the study of nonlinear systems extended in one spatial dimension has received a great deal of attention, as scientists in many fields realized that the time-honored method of linearizing nonlinearities that occur in their equations omits phenomena which are of great importance, often fundamental to the problem under consideration. One of these areas, to which much effort has been devoted, is that of *nonlinear waves* [15, 41, 63]. Here, the existence of special *solitary wave* solutions, that is, localized solutions which depend on x and t only through the argument $x-vt$, has indeed had a great impact on the scientific community. Of special interest is a particular type of solitary wave called a *soliton*, which

*Received by the editors February 24, 1997; accepted for publication (in revised form) September 26, 1997. This work was supported by the Comisión Interministerial de Ciencia y Tecnología of Spain through grant Mat95-0325, by the Ministerio de Educación y Cultura of Spain through "Acciones Integradas Hispano-Alemanas" and grant PB96-0119, and by the United States Department of Energy.

http://www.siam.org/journals/sirev/40-3/31741.html

†Grupo Interdisciplinar de Sistemas Complicados, Departamento de Matemáticas, Universidad Carlos III de Madrid, c/ Butarque 15, 28911 Leganés, Madrid, Spain and Theoretical Division & CNLS, MS B258, Los Alamos National Laboratory, Los Alamos, NM 87545 (anxo@dulcinea.uc3m.es).

‡Theoretical Division & CNLS, MS B262, Los Alamos National Laboratory, Los Alamos, NM 87545.

has the additional property that its shape and velocity are preserved asymptotically upon collisions with other solitary waves.

Although the concept of solitary waves dates back to the now famous (1844) report by John Scott-Russell [57] of his chase of a "wave of translation" along a shallow canal, the first evidence that mathematical models could have soliton solutions had to wait until the numerical investigation of the sine-Gordon (sG) equation in a field theory context by Perring and Skyrme in 1962 [44]. In 1965, Zabusky and Kruskal published results of a similar numerical investigation [67],[1] this time using the Korteweg–de Vries (KdV) equation with quite different physical motivations. In both cases, the simulations showed that after colliding, two solitary waves emerged with the same shape and velocity that they had long before they interacted. Subsequent analytical work produced *multi*soliton solutions which described the collisions with the help of Bäcklund transformations [41], a development which eventually led to the famous inverse scattering transform (IST) [1, 41]. By means of the IST technique, one could actually find action-angle variables for the sG and KdV equations; soon, other integrable models including the nonlinear Schrödinger (NLS), Boussinesq, and modified KdV equations were discovered, adding to the extensive set of evolution equations now known to yield solitons [1, 15, 41]. In addition, many nonintegrable models, not amenable to the beautiful IST machinery, were also found in which solitary waves exist and have "nearly" elastic collisions, such as the so-called ϕ^4 equation [10, 11, 15, 48].

It is of course the application of these equations which is of most value to the physicist, engineer, biologist, etc. The observation by Scott-Russell (an engineer himself) of a solitary wave in water was the first study of a soliton-bearing physical system. Since then, solitary waves and their corresponding equations have found their way into many modern applications. Indeed, there are very many systems whose behavior is approximated by the completely integrable, soliton-bearing, nonlinear partial differential equations (PDEs), such as long Josephson junctions (sG equation, [5]), optical fibers (NLS equation, [25]), or, on the nonintegrable side, materials with structural phase transitions (ϕ-four equation, [35]), to name a few. However, more often than not, integrable and quasi-integrable equations describe a highly idealized version of the system of interest. The applied scientist, when pursuing a more realistic analysis of the problem, is almost always forced to add new terms to the original equation, usually rendering it nonintegrable. Therefore, one must develop perturbation schemes to obtain approximate solutions. Several such schemes have been proposed in recent years, and we will briefly review them in section 2.

A number of the above-mentioned perturbation theories are based on the fact that although one cannot obtain an exact solution merely by a specification of the motion of the solitary waves, such a description can often provide a good first approximation [8]. By concentrating on the motion of the solitons themselves instead of trying to follow the solution in its full detail, one can achieve a drastic reduction in the dimensionality of the system; i.e., one can perform a nonlinear mode reduction from the originally infinite-dimensional problem to a low dimensional system of ordinary differential equations (ODEs) for the so-called collective coordinates. It is the *first purpose of this paper to describe such theories* through their application to a specific problem, the *sG equation with a spatially periodic perturbation*, a problem which has been understood by means of collective coordinate techniques in the last few years. We hope that this example and the comparison of the results obtained by

[1] This is the paper in which the word "soliton" was proposed to name these solitary waves.

different perturbative approaches will demonstrate that collective coordinate theories are one of the very few robust and practical techniques for general nonlinear PDEs supporting solitons or solitary waves. To this end, section 3 presents a thorough picture of the illustrative problem, beginning with a summary of the previous work, and proceeding to a detailed exposition of the calculations and results. Also included at the end of section 3 is an account of very recent collective coordinate results on this problem. Appendix A collects, in an abbreviated manner, a number of examples of the application of collective coordinate theories in other contexts, including cases when they do not work.

The problem we discuss in this paper is not chosen at random. On the contrary, the periodically perturbed sG equation will also allow us to achieve the *second aim* of this work, namely *to introduce a phenomenon, which we term length-scale competition*, which is of nonperturbative nature and likely to arise in all instances where there are two or more particular scales in the problem competing with each other, leading to an instability. Whereas such a concept is not restricted to soliton-bearing equations, length-scale competition arises particularly naturally in those equations when perturbed by time-dependent or spatially dependent terms with a specific length scale (or scales). The reason is that solitons or solitary waves already introduce one scale in the problem (their "size" or "width," determined by the "nonlinearity" strength), and therefore competition between the nonlinearity and perturbation ("disorder") scales can take place. In the example of section 3, those scales will be the sG soliton length and the wavelength of the perturbation. Appendix B summarizes some other instances of this phenomenon to underline its generality as well as to present a few other aspects. Being a non-perturbative feature, the study of length-scale competition is carried out mostly by means of computer simulations; appendix C is devoted to the numerical procedures we have used. Finally, we close the body of the paper with a brief recapitulation, a few comments about related works, and a discussion of prospects and open questions which can be of interest for both an applied mathematics and a more general audience.

2. Soliton perturbation theories. As noted above, in spite of the fact that integrable equations are not likely to govern most real systems and applications, soliton-bearing equations often serve as a starting point to which perturbations can be added to more closely mimic the problem of interest. The addition of such perturbations will certainly modify the propagation of the solitons and will quite likely produce some "phonons" or "radiation," i.e., (quasi-linear) deformations of the background shape of the solution on top of which solitons propagate, as well as shape deformations of the solitons themselves—hence the importance of developing perturbation methods which not only predict the motion of solitons but also account for any phonons emitted and any effect they may have on the motion of the solitons and on the asymptotics of the solution as a whole. The perturbations which modify the otherwise straightforward motion of solitons come in many varieties, depending on the specific effect one needs to include in the model under consideration.

To clarify the ideas and the corresponding type of perturbations we have in mind, consider the model we will be mostly dealing with, namely the sG equation, which reads (subindices mean derivative with respect to the variable, and $u \equiv u(x,t)$)

$$u_{tt} - c_0^2 u_{xx} + \omega_0^2 \sin u = 0, \tag{2.1}$$

where c_0 and ω_0 are a velocity and a frequency characteristic of the particular physical context. To be specific, we will consider the familiar example of the long Josephson

junction [5, 38], which consists of two identical superconducting strips separated by a thin dielectric layer. Then x is the long direction of the junction (the width of the junction is neglected), t is time, u is the magnetic flux in units of the flux quantum or fluxon, c_0 is the Swihart velocity, and ω_0 is the Josephson plasma frequency. In deriving (2.1), a number of assumptions have to be made, most notably all dissipative effects and imperfections in the transmission line are neglected. If those are included to make the description of the Josephson junction realistic, (2.1) becomes

$$u_{tt} - c_0^2 u_{xx} + \omega_0^2 \sin u = -\alpha u_t + \beta u_{xxt} - \gamma - \omega(x) \sin u, \tag{2.2}$$

where the perturbative terms represent, respectively, shunt loss due to quasi-particle tunneling, dissipation due to the surface impedance of the superconducting films, a spatially uniform bias current provided by an external source, and inhomogeneities of the insulating layer leading to local modifications of the Josephson frequency. These are the most relevant factors affecting the ideal description of (2.1), and (2.2) is already a very good description of the junction dynamics. However, it is possible to include more subtle effects by adding suitable additional perturbation terms (see, e.g., the exhaustive list in [31]).

Having mentioned in section 1 some of the elegant methods for studying integrable soliton-bearing systems, one might expect that they could serve as a basis for perturbation theories. Just such a method was applied by McLaughlin and Scott [38] to study (2.2), by linearizing about a (nonlinear) zeroth-order solution and writing the corrections in terms of a Green function. To ensure that the expansion is valid for times of the order of the inverse perturbation strength, one finds that the unperturbed zeroth order soliton is not a valid starting point. However, allowing its parameters (such as position and velocity) to depend slowly on time resolves the problem because then a secularity condition can be satisfied yielding equations of motion for the soliton position and velocity. Next one solves for the radiation terms using the Green function, a step where the IST is required and herein lies the major drawback of this method: Although IST is a very powerful method, it requires a high degree of mathematical sophistication. However, there are advantages to this method, one of them being that it applies to multisoliton waveforms. In any case, the necessity of the IST confines this technique to integrable models as starting points. A similar perturbation theory, based on the change in time of the infinite number of conserved quantities of the system, was developed by Kaup and Newell [28], yielding basically the same results as the approach of McLaughlin and Scott. Several other schemes have been worked out on the basis of the IST for the unperturbed problem; a comprehensive review of these is given in [31] so we will not dwell further on them here.

The major limitation of IST-based perturbation theories is the fact that they can only be used when the unperturbed equation is integrable, and, further, they are problem-dependent in so far as the Lax pair [1] and the IST itself are different for every equation. Therefore, even if the general ideas for IST perturbative calculations were to apply to any originally integrable problem, they could eventually lead to intractable mathematical complexities. One way out of this restriction is the use of "naive" perturbative expansions about any known solution of the unperturbed equation, what is usually called a "direct perturbation method." One of the first such methods in this context was presented by Fogel et al. [21]. In fact, they did not use a perturbative expansion but rather a splitting of the full solution of the perturbed problem into two contributions, a zeroth-order or soliton one plus a phonon part, the latter being assumed to be of the order of the perturbation strength. This technique

is fully described in section 3.2.2, to which the reader is referred for details. Let us just note at this point that, whereas the technique is simple and easy to apply to any soliton-bearing equation, it can lead to divergences for some typical perturbations. As in the McLaughlin-Scott approach, one then needs to introduce time-dependent parameters in the zeroth-order solution to take care of secular terms if present. Another variant of this technique that can be used when the perturbation induces a natural separation of time or length scales combines the soliton-phonon splitting with multiple scale analysis. The phonon contribution corresponding in this context to a "fast" part, which affects the zeroth-order term only through averages [34]. Of course, more involved perturbative expansions have been proposed and used (see, for instance, [4],[2] or [29] for a multiple-scale version), but aside from the fact that they almost invariably suffer from divergence problems, they pose serious convergence questions about which very little can be said rigorously. However, if used judiciously and combined with numerical simulations to verify the results, these techniques are often the only available perturbative tool to which one can resort; hence their importance.

Although not explicitly stated in the previous paragraphs, the perturbative methods of McLaughlin and Scott and of Fogel et al. utilize *collective variables or coordinates* when allowing the position and/or other soliton parameters to evolve in time. In their approaches, this was partly a technicality to remove divergences in their expansions, but it also provided useful information on the effect of the perturbation on the soliton itself, although not about the whole solution. However, in many instances it is known that the phonon-like correction is negligible, either because one can show its smallness through one of the above approaches or because numerical simulations indicate that this is indeed the case. This amounts to saying that in those situations the perturbation affects only (to be precise, mostly) the soliton motion, leaving its shape practically undisturbed, and therefore collective coordinates are enough to describe the problem under consideration. This is the origin of the collective coordinate approach to perturbed soliton problems: One can *assume* that radiative or phonon-like corrections are small and concentrate on deriving the equations of motion for the soliton, usually by much simpler means than in the above cases, which is the main virtue of such a technique. Because of its simplicity, this technique can be always used and the applicability of its results checked a posteriori. The success of the collective coordinate approach is that it usually yields quite accurate predictions, as we will see.

There are several different practical procedures to implement the idea of collective coordinates. We will be using some in section 3, and here we will summarize others for completeness. The choice between these procedures is often a matter of taste or amenability of the corresponding calculations. To begin with, using again the sG system as an example, we know that an exact soliton (also termed *kink* because of its topological shape) solution has a parameter x_0 which locates its center, i.e., it can be written as $u_k \equiv 4\tan^{-1}[\exp(x-x_0)]$, x_0 being a constant if the kink is at rest or time dependent if it is moving. Allowing it to depend on time one can define a Lagrangian

$$L(x_0, \dot{x}_0; t) \equiv \int_{-\infty}^{\infty} dx\, \mathcal{L}[u_k(x, t : x_0)], \tag{2.3}$$

where $\mathcal{L}[u(x, t : x_0)]$ is the Lagrangian of the perturbed sG equation. This procedure was first proposed by Rice and Mele [49], although a more rigorous formulation has

[2]The review [4] is particularly interesting because it contains a number of techniques useful to deal with stochastic soliton-bearing equations, a topic which is outside the scope of the present work but whose importance is growing rapidly. See also [71] on this subject.

been recently put forward by Caputo et al. [12] to remove singularities appearing in certain cases.

Another example of a collective coordinate technique is the work of Bergman et al. [3], who used the fact that the derivative of the soliton waveform is a well-localized function in space to define as their collective coordinate $Q \equiv \frac{1}{2\pi}\int_{-\infty}^{\infty} dx x u_x$, along with a momentum, which can be shown to be canonically conjugate to Q, $P \equiv \int_{-\infty}^{\infty} dx \Pi u_x$, Π being the momentum conjugate to u. Equations of motion can be straightforwardly derived for these quantities from their definition and the perturbed sG equation, and they lead to the conclusion that kinks behave like classical "relativistic" particles. Note, however, that this choice of collective coordinate includes a contribution from the phonon part of the solution through the presence of u_x in the integral. In order to deal properly with this problem, one would have to clearly identify a soliton and a phonon component. Such separation was accomplished exactly by Tomboulis [62] while retaining the canonical properties of the approach; the reader is referred to the original work, as well as to further elaboration in [9], for details which we omit here in view of their length.

As one last example, equations of motion for collective variables can be derived from conservation laws of the system, as was suggested by Pascual and Vázquez [43] (see also [33] for a pedagogical presentation). Take for instance the momentum of the sG equation, $P \equiv \int_{-\infty}^{\infty} dx\, u_t u_x$; this quantity, conserved in the unperturbed evolution, will change in time if a perturbation is added in a way that can be obtained from the perturbed equation itself. On the other hand, for an unperturbed kink moving with velocity v, $P(v) = 8v(1-v^2)^{1/2}$; for the collective coordinate analysis we now assume v is a function of time and compute the time derivative of $P(v)$. The constraint that the two forms of computing this time derivative should be consistent leads to a differential equation for v and hence for the soliton position. As stated, we will discuss below other ways to perform this mode reduction from the PDE to collective coordinate ODEs, and there are also more approaches we do not describe here (e.g., inserting the ansatz for the solution directly in the equation). The important issue, which we are going to address now, is how good these techniques are when used in practice, and how their results compare to more sophisticated approaches. This is the subject we discuss in the next section.

3. sG kinks on spatially periodic perturbations. The problem we are going to address is that of (2.2) with $\alpha = \beta = \gamma = 0$ and $\omega(x) = \epsilon \cos k(x)$. Properly nondimensionalized, the *periodically perturbed sG equation* is given by

$$u_{tt} - u_{xx} + [1 + \epsilon \cos(kx)] \sin u = 0. \tag{3.1}$$

Such an equation has a number of applications, the most important of them probably being that it models a long Josephson junction with modulated critical current, which can be realized experimentally by periodically changing the insulator layer thickness [23]. Mkrtchyan and Shmidt [40] were the first ones to propose this model, and subsequently they and Malomed and Tribelsky [36] studied the question of whether kinks can propagate freely in such a system; after this last paper, which included the damped [$\alpha \neq 0$ in (2.2)] case, appeared, the problem was regarded as basically solved. To begin our discussion of (3.1), we will first present a short summary of these authors' work. The reader is referred to the original papers [36, 40] for details.

Mkrtchyan and Shmidt [40] worked out a Green-function perturbation technique (GFPT). They derived a linearized equation for the first order correction to a kink moving with constant velocity, computed the Green function corresponding to its

homogeneous version, and then used it to obtain the desired correction by integrating the source term with that Green function. They then noticed that radiation appeared only above a critical kink velocity $v_{\rm thr} = (1+k^2)^{-1/2}$. At that particular velocity, the correction diverges, and the authors explain that their calculation becomes invalid in that region, as, of course, it assumed the correction was small.

The approach of Malomed and Tribelsky [36] was quite different. They resorted to a version of the inverse scattering perturbation theory (ISPT) which we have referred to in section 2 [31]. The basic idea of this type of ISPT is that, if the amount of radiation emitted by the kink is small, as it should be if the perturbation is small, then the spectral density of the emitted energy can be computed following a Taylor expansion, and the total radiated energy is then derived by integration over all modes. Again, the result was that there was a critical velocity $v_{\rm thr} = (1 + k^2)^{-1/2}$ such that kinks traveling with velocities $v < v_{\rm thr}$ did not emit any radiation at all, whereas in the opposite case the amount of emitted radiation decreased as $v \to 1$, diverging when $v = v_{\rm thr}$. Within the framework of ISPT, Malomed and Tribelsky [36] were also able to show that dissipation could play a regularizing role, suppressing the divergence. As the results in [40] agreed with those in [36], the existence of this threshold for radiation with its associated divergence seemed plausible.

When discussing the early results [36, 40], it is important to have in mind that those authors' main purpose was to establish the proper foundations for a perturbative theory for solitons, and hence they pay less attention to the physical interpretation of their finding, i.e., the question of the meaning and origin of the divergence was not addressed. In fact, an unexplained point arises already from ISPT, which allows computation of the radiation nature. When this is done in our case, the radiation wavenumbers turn out to be related to the perturbation wavenumber by a complicated equation (see, e.g., [31]), which, in particular, implies that radiation is emitted with a non-intuitive wavenumber k^{-1} at the divergence. This prediction is difficult to understand physically but, if true, its origin must come from the wave nature of kinks and, consequently, such result would not be attainable within a collective coordinate approach.

3.1. Kink propagation: The threshold problem.

3.1.1. Numerical results. As we have just seen, the periodically perturbed sG equation was seemingly understood, although the results presented a few puzzles. In order to clarify these, and having in mind that no numerical verification of the perturbative results had been carried out, we revisited the problem [52], beginning by performing a number of numerical simulations (see Appendix C for a brief summary of the techniques we used) looking for the proposed threshold. We performed a careful search, paying attention to the fact that the predicted value was a first order calculation, and that it might not be quantitatively accurate. On the other hand, the finite width of the simulated system may also be of relevance at this point, as its radiation spectrum structure is not identical to that of the continuum, infinite system (in particular, the lowest frequency in the model is restricted to be $\omega^2_{min} = 1+(2\pi/L)^2$, L being the length of the system). Hence, we monitored the amount of radiation emitted by the kink by making simulations with many different initial conditions, sweeping a range of initial velocities; if there were a threshold somewhere, there should be a change in the radiative power of the kink as it moved through it. The result was negative: No evidence for a threshold was found, even when the search was performed for a large range of initial velocities with a resolution of 10^{-2} for some choices of k. Examples of the outcome of the simulations are shown in Fig. 3.1 for three values of

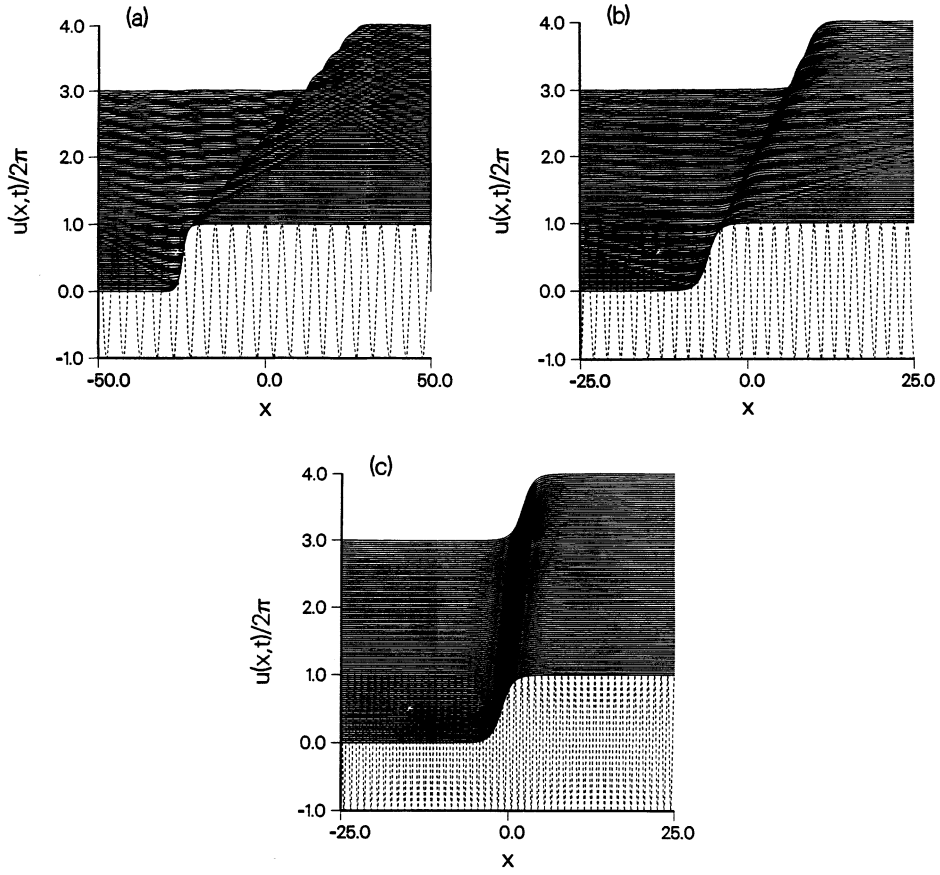

FIG. 3.1. *Absence of radiative divergence for kinks propagating in the spatially periodic sG model. Parameters are:* (a) $k = 2\pi/5$, *initial velocity* $v = v_{\rm thr} = 0.387726\ldots$; (b), $k = \pi$, *initial velocity* $v = v_{\rm thr} = 0.091999\ldots$; (c), $k = 2\pi$, *initial velocity* $v = v_{\rm thr} = 0.024704\ldots$ (*corresponding wavelengths are* (a) 1, (b) 2, (c) 5). *In all three cases,* $\epsilon = 0.4$. *The amplitude of the emitted radiation is very small; due to the periodic boundary conditions, it can be seen reentering the simulation interval without any appreciable interaction with the kink. Only half of the simulation interval is shown in plots* (b) *and* (c) *to enlarge details. Time increases upwards with final time* $t = 100$. *The potential is indicated by the dashed line (amplitude not to scale).*

the potential wavelength, of the order of (a) and smaller (b), (c) than the kink width (~ 6 in our dimensionless units) at $v = v_{\rm thr}$. It has to be stressed that the predicted divergence does not depend on the strength of the perturbing potential, ϵ, but we also tried to make the effect more visible by increasing this parameter. Indeed, in Fig. 3.1, $\epsilon = 0.4$, a value that is not very small, and the kinks seem unaffected except for a small amount of radiation and an oscillatory motion superimposed on their trajectory. It is interesting to note that the kink traveling on the short wavelength potential (c) appears not to be affected at all. On increasing ϵ further, trapping behavior takes place, i.e., kinks are trapped by the potential and cannot propagate, but there is no strong emission of radiation (for an example, see Fig. 3.3(b), which will be discussed later). Actually, this trapping can be of two very different kinds, as we will discuss below. Another interesting remark is that we also observed that kinks always emit radiation, even when moving at a very low velocity, far below the predicted threshold (note that complete suppression of radiation had been predicted in this region; we

will come back to this point in section 3.4). It thus becomes evident that the features of kink propagation on periodic potentials are qualitatively different from the above perturbative analytical results. Complementary numerical simulations on a similar perturbation of the ϕ^4 problem [16] seem to confirm the absence of this divergence. We will elaborate more on this when discussing our results on the threshold question in section 3.2.3.

3.1.2. Theory. In order to gain insight into the numerical observations, we resorted to the perturbative approach of Fogel et al. [21]. As announced above, we will describe the computation in detail because of its wide applicability.

To begin with, we perform a Lorentz transformation and rewrite (3.1) in the rest frame of the soliton (i.e., the reference frame moving with the speed of the unperturbed soliton, v)

$$u_{tt} - u_{xx} + \{1 + \epsilon \cos[k\gamma(x + vt)]\} \sin u = 0, \tag{3.2}$$

with $\gamma \equiv (1 - v^2)^{-1/2}$ the Lorentz factor. Here we consider $\epsilon \ll 1$, so the perturbative term may be treated by assuming a solution of the form

$$u(x,t) = u_v(x) + \epsilon u^{(1)}(x,t), \tag{3.3}$$

where $u_v(x) \equiv 4 \tan^{-1}(e^x)$ is, as before, the unperturbed sG kink, written in its own rest frame and centered at $x = 0$. For completeness, we now recall how the most appropriate basis in which to expand $\epsilon u^{(1)}(x,t)$ is obtained. Introducing the *Ansatz* (3.3) in Eq. (3.2) without the perturbation term, linearizing in the small quantity $u^{(1)}(x,t)$, and separating time and space by introducing $u^{(1)}(x,t) = f(x)e^{-i\omega t}$, we are left with the following eigenvalue problem for $f(x)$:

$$\left[-\frac{d^2}{dx^2} + \left(1 - 2\mathrm{sech}^2 x\right)\right] f(x) = \omega^2 f(x). \tag{3.4}$$

This is a well known, analytically solvable eigenvalue problem [20, 22]; there exists exactly one bound state, with $\omega_b = 0$, and a continuum of scattering states with $\omega_\kappa^2 = 1 + \kappa^2$; the corresponding normalized eigenfunctions are

$$f_b(x) = 2 \,\mathrm{sech}\, x \tag{3.5}$$

$$f(\kappa, x) = \frac{1}{\omega_\kappa \sqrt{2\pi}} e^{i\kappa x} \left(\kappa + i \tanh x\right). \tag{3.6}$$

These eigenfunctions have clear physical meaning. The bound state $f_b(x)$ is associated with the zero-frequency (Goldstone [48]) translation mode of the soliton, whereas the continuum eigenfunctions $f(\kappa, x)$ are the radiation modes (see [21] for a detailed discussion). It is interesting both for understanding the connection to collective coordinates and for pedagogical purposes to clarify the above claim about $f_b(x)$. For this, note that $f_b(x) = u_v'(x)$; therefore, the addition of a small amount of this bound state has the effect of translating the kink, i.e., $u_v(x) + \epsilon f_b(x) = u_v(x + \epsilon) + O(\epsilon^2)$, explaining the terminology "translation mode."

The functions $f_b(x)$ and $f(\kappa, x)$ form an orthogonal basis, since the corresponding operator is self-adjoint. In terms of this basis, the first-order correction can be split into two parts, namely,

$$u^{(1)}(x,t) = u^{(\mathrm{trans})}(x,t) + u^{(\mathrm{rad})}(x,t), \tag{3.7}$$

where

$$u^{(\mathrm{trans})}(x,t) = \frac{1}{8}\phi_b(t) f_b(x), \tag{3.8}$$

$$u^{(\mathrm{rad})}(x,t) = \int_{-\infty}^{\infty} d\kappa\, \phi(\kappa,t) f(\kappa,x), \tag{3.9}$$

where, according to the earlier comment on the translation mode, $\phi_b(t)$ is simply the displacement of the soliton in time, i.e., the coordinate of its center; herein lies the connection to collective coordinate approaches.

To find the amplitudes $\phi_b(t)$ and $\phi(\kappa,t)$, one again introduces the ansatz (3.3) in (3.2), linearizes and Fourier transforms in time; subsequent projection yields

$$\ddot{\phi}_b(t) = 4\int_{-\infty}^{\infty} dx\, \cos[k\gamma(x+vt)]\frac{\sinh x}{\cosh^3 x}, \tag{3.10}$$

$$\ddot{\phi}(\kappa,t) + (1+\kappa^2)\phi(\kappa,t) = 2\int_{-\infty}^{\infty} dx\, \cos[k\gamma(x+vt)]\frac{e^{-i\kappa x}(\kappa - i\tanh x)}{\sqrt{2\pi(1+\kappa^2)}}\frac{\sinh x}{\cosh^2 x}. \tag{3.11}$$

It now remains to solve (3.10)–(3.11) and invert the various transforms needed to arrive at them. In the following, we discuss translation and radiative parts in (3.7) separately. Let us start with the simplest one, i.e., the translation mode contribution. Note that (3.10) is, after performing the integration, nothing but Newton's law for a time-dependent force. Its solution may be readily found, and finally one obtains

$$u^{(\mathrm{trans})}(x,t) = \frac{\pi}{2v^2\sinh(k\gamma\pi/2)}\sin(k\gamma vt)\,\mathrm{sech}\, x. \tag{3.12}$$

Recalling that we are working in the unperturbed soliton reference frame, this is a localized oscillatory motion superimposed on its otherwise constant trajectory. Now, let us remark that the prefactor implies that short wavelength ($k \to \infty$) perturbations will have no effect on the motion of the center of the soliton, which is also in good agreement with our simulations. This behavior can be understood in terms of a "smoothing" of the potential: The kink, having a width much larger than the perturbation wavelength, experiences only an effective averaged force, whose amplitude vanishes exponentially for large k. The name "renormalized particle" has been coined to describe this limit because of such an averaging phenomenon. We will pursue further the particle picture in section 3.2; by now, our main goal is to understand the threshold problem, so we need to examine the radiation part.

Equation (3.11) for the κ-mode radiative contribution can also be solved. After computing the integral in the right hand side of (3.11), one is left with Newton's law for a forced harmonic oscillator. This allows the determination of $\phi(\kappa,t)$, and substitution of it in (3.9) to find the total radiative contribution:

$$u^{(\mathrm{rad})}(x,t) \equiv \frac{1}{4}\left[\tanh x - \frac{\partial}{\partial x}\right] \times \int_{-\infty}^{\infty} d\kappa \frac{1+\kappa^2-k^2\gamma^2}{(1+\kappa^2)(1+\kappa^2-k^2\gamma^2v^2)} \times \left[\frac{e^{ik\gamma vt}}{\cosh[\pi(k\gamma-\kappa)/2]} + \frac{e^{-ik\gamma vt}}{\cosh[\pi(k\gamma+\kappa)/2]}\right] e^{i\kappa x}. \tag{3.13}$$

It is possible to deal with the integral in (3.13) in the complex plane: When $x > 0$, in the upper half plane, and when $x < 0$ in the lower half plane. The pole structure of the integrand will completely determine the total radiative contribution. In particular, we will see that radiation only appears for some special values of the system parameters.

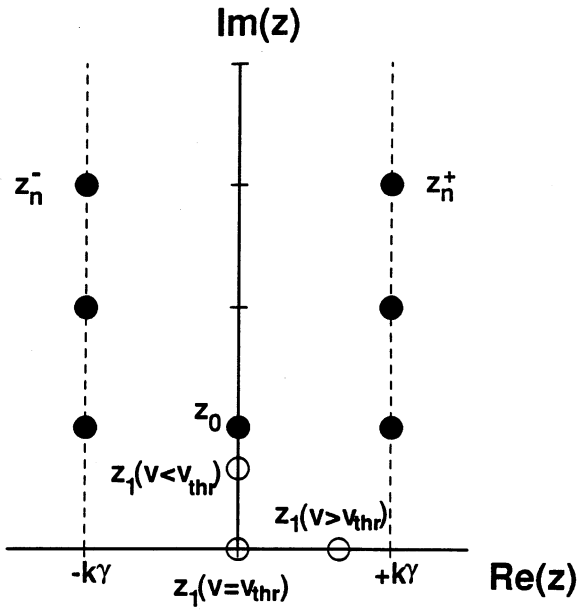

FIG. 3.2. *The pole structure of the radiation contribution. Filled circles mark the location of the poles which give rise to corrections localized around the soliton. Empty circles denote the locations of pole z_1 as the velocity changes. Only when z_1 becomes real ($v > v_{\rm thr}$) does it originate propagating wavelike corrections. See text for further explanation.*

We take $x > 0$ in what follows (the opposite case is treated in the same way). Accordingly, the integral has to be analyzed in the upper half complex plane. The pole structure of the integrand is depicted in Fig. 3.2. All poles are simple, and their locations are $z_0 \equiv +i$, $z_1 \equiv i\alpha \equiv +i\sqrt{1-k^2\gamma^2v^2}$, and $z_n^{\pm} \equiv \pm\kappa\gamma + i(2n+1)$, n being a non-negative integer. For the sake of clarity we now treat each pole separately.

i. The first pole, $z_0 = +i$, is constant, and does not change when the system parameters change. Since this pole is purely imaginary, it is immediately seen that the contribution of the residue at z_0 is exponentially localized around the kink center. This term does not give rise to any radiation, but rather to time-dependent corrections of the kink shape.

ii. The family of poles $z_n^{\pm}$ depends on the perturbation wavenumber k and on the kink velocity through the Lorentz factor γ. However, they always have a positive imaginary part, thus leading again to exponentially localized contributions. Therefore, the $z_n^{\pm}$ poles also do not produce any true radiative correction.

iii. The remaining pole is the key one. If $\alpha^2 \equiv 1-k^2\gamma^2v^2 > 0$, the same reasoning applied to the other poles holds, and there is no radiation. It is worth mentioning that localized oscillations around the kink center, predicted from the contributions of z_0, z_1 (α real), and $z_n^{\pm}$, were already evident in our numerical simulations, as shown in Fig. 3.1. For fixed k, as v increases, the pole moves down the imaginary axis, and at the critical value $v_{\rm thr} \equiv (1+k^2)^{-1/2}$ it lies at the origin of the complex plane. For kink velocities $v > v_{\rm thr}$ the pole is purely real, and then it *does* give rise to a radiative contribution, whose form is given by (with $\beta \equiv \sqrt{k^2\gamma^2v^2-1}$ a real number)

$$u_\beta^{(\rm rad)} = \frac{\pi}{4\gamma^2v^2}\left(1-\frac{i}{\beta}\tanh x\right)\left[\frac{e^{i(k\gamma vt+\beta x)}}{\cosh[\pi(k\gamma-\beta)/2]}+\frac{e^{-i(k\gamma vt-\beta x)}}{\cosh[\pi(k\gamma+\beta)/2]}\right]. \tag{3.14}$$

This expression tells us that radiation occurs whenever β is real ($v > v_{\rm thr}$), and this radiation is the superposition of two linear waves of different amplitudes, traveling in opposite directions but with the same phase velocity.

3.1.3. Discussion. To this point, it appears that our perturbative calculation leads exactly to the same (numerically found to be wrong) prediction as those in [36, 40], namely that there is a critical velocity $v_{\rm thr} \equiv (1+k^2)^{-1/2}$ below which kinks do not radiate and above which they do. At that precise velocity, the amplitude of the emitted radiation diverges; notice that β vanishes as v approaches $v_{\rm thr}$ from above and consequently the prefactor in (3.14) tends to infinity. However, this apparent equivalence is not so. The crucial difference arises when one examines more carefully (3.14): As $v_{\rm thr}$ is approached, not only the amplitude of the emitted wave diverges, but also its wavelength $2\pi/\beta$. Then, we are faced with something similar to an "infrared" divergence, and usually those do not have a real physical meaning. We will show immediately that this is indeed the case here, but let us first comment on the reasons why our calculation provides us with this physically relevant result that was not transparent in the previous approaches. As to the GFPT computation, Mkrtchyan and Shmidt [40] compute the first-order correction to the field much as we do here (actually the two approaches are basically the same in the beginning), but they do not use the natural translation mode-radiation basis, so they cannot separate the different contributions and are therefore led to an expression that they cannot analyze in detail; as we already pointed out, they merely remark that their calculations are invalid in the vicinity of the divergence, as they assumed the correction should be small. On the other hand, ISPT [36] yields a different result than ours despite using a suitable basis, because the integration over κ is made in an incoherent fashion, i.e., integrating over emitted *energy* instead of emitted *amplitude* (we notice in passing that many ISPT results are obtained by this same means, which casts some doubt on their interpretations also). When the integration over radiation modes is made coherently as shown here, the correct result turns out to be different due to the superposition of modes.

Now that we have a reliable perturbative calculation, we need to understand what is the nature of the divergence. To make progress, it is important to turn to the form of our starting (3.1) *with dimensions* as in (2.1), namely,

$$u_{tt} - c_0^2 u_{xx} + \omega_0^2[1+\epsilon\cos(kx)]\sin u = 0, \tag{3.15}$$

where c_0 and ω_0 are a velocity and a frequency characteristic of the particular physical context. Redoing the calculations with dimensions transforms the divergence condition $k\gamma v_{\rm thr} = 1$ into $k\gamma_0 v_{\rm thr} = \omega_0$ [$\gamma_0 = (1 - v^2/c_0^2)^{-1/2}$]. This immediately clarifies what happens: The divergence occurs when the velocity of the kink is such that the time it takes to travel through a wavelength of the potential, $T_0 = \lambda/(\gamma v_{\rm thr})$, $\lambda = 2\pi/k$, is exactly the period of the lowest frequency phonon, $T_0 = 2\pi/\omega_0$. If the velocity is lower than $v_{\rm thr}$, the kink will not be able to excite phonons, whereas when its velocity is higher it can, and will subsequently radiate. At $v_{\rm thr}$, the excited radiation is that of the lowest phonon, and it has infinite wavelength and velocity, as predicted by our calculation. This physical picture of kinks exciting radiation according to the frequency of their propagation through a potential wavelength becomes therefore the likely candidate to explain the divergence. On the other hand, now it also becomes clear that there is a divergence of the energy at $v_{\rm thr}$: It diverges because of the infinite contribution arising from the infinite wavelength mode when integrated over the whole x axis. This agrees with GFPT and ISPT results, whose only shortcoming was not to specifically identify the mode responsible for the divergence.

In spite of this clarification, the most significant question is not yet answered: Why is it that numerical simulations do not agree with this calculation, which seems to allow for a simple and physically reasonable interpretation? Examining Fig. 3.1 again, it is easy to realize that the flaw of the perturbative calculation is at its very root: We are computing first order corrections around a kink moving at a *constant velocity* v, and this condition never holds. Whatever the starting position of the kink, it will behave like a particle in the sense that it will be accelerated or decelerated depending on whether it travels toward a minimum or a maximum of the potential. In fact, the translation mode correction itself is describing this: The kink velocity, in its reference frame, is not zero but rather it oscillates between positive and negative values. It is not a surprise, then, that first the resonance condition we have obtained is never matched, and second that the kink emits radiation at any velocity, because it is accelerating or decelerating. Of course, we should note that this is a perturbative calculation including only first-order terms; the possibility still remains that the divergence is suppressed by higher-order nonlinearities. Even so, we believe that the explanation we have provided here points to the crux of the solution of this dilemma, a conclusion reinforced by the fact that our results are likely to be general for kink-bearing models in view of the related results of [16] on the spatially periodic perturbed ϕ^4 model. Some remarks are in order regarding this problem: The same kind of divergence is predicted by a direct perturbation theory similar to the one used here and, again, numerical simulations show evidence of the unphysical character of the divergence. It can be seen from Fig. 4 of [16] that as the velocity of a decelerating kink passes through the threshold nothing special occurs. Most of the reasoning we have used in the present study applies also to that work (with an additional feature coming from the finite frequency shape mode of the unperturbed ϕ^4 kink [20]), thus reinforcing the generality of our results. As a matter of fact, recent work of Willis [64], which appeared while we were writing this article, fully confirms the picture we are providing here, as we discuss in section 3.4, where we review the newest results on this problem.

3.2. Collective coordinate approach. The above numerical results and the subsequent perturbative calculation strongly suggest that, contrary to the expectation of non-particle-like behavior arising from previous research [36, 40], sG kinks behave as point-like particles in the presence of a periodic parametric potential like the one we deal with here. Therefore, it is natural to try to describe those results by means of the collective coordinate formalism. Indeed, this is a good example to appreciate the advantages of this technique because we can compare with the results of the previous section and with numerical simulations.

As we have already seen, the basic idea of the collective coordinate formalism is very simple: To reduce a complicated problem with an infinite number of degrees of freedom, posed in terms of a PDE, to a much less complex problem with a few degrees of freedom described by ODEs. It is known by now that there are a number of ways to achieve this, and different quantities can be chosen to play the role of collective coordinates describing the motion of the nonlinear excitation as a whole. We will now present yet another alternative which is the most direct and physically motivated approach. Again, we simply consider the kink center as our collective coordinate for the kink, and assume that its motion will be governed by an effective potential that can be computed by integrating the perturbative contribution to the hamiltonian over the kink profile, i.e.,

$$V_{\text{eff}}(x_0,t) = \epsilon \int_{-\infty}^{\infty} dx\,[1-\cos u_v(x-x_0,t)]\cos kx, \tag{3.16}$$

where $u_v(x - x_0, t)$ now denotes a kink moving with constant velocity v and centered at x_0. This integral can be easily evaluated and yields

$$V_{\text{eff}}(x_0, t) = 2\epsilon \frac{k\pi}{\gamma^2 \sinh(k\pi/2\gamma)} \cos[k(x_0 + vt)]. \tag{3.17}$$

From (3.17) we see that the potential experienced by the particle equivalent to the kink is basically the same perturbation potential that appears in the PDE (3.1), although the prefactor in front of it is quite complicated. The simplest dependence of this prefactor is on the wavenumber. It can be seen immediately that when $k \to 0$ (long wavelength limit) the effective potential prefactor reduces to $4/\gamma$ and subsequently V_{eff} comes closer to the perturbative potential; in the opposite limit, $k \to \infty$, the sinh term makes the effective potential vanish exponentially. This is in agreement with what we have learned so far: Looking at Fig. 3.1, it can be seen that the short wavelength potential has no effect on the kink (c), whereas the motion on long wavelength perturbations resembles that of a particle in the bare potential. As we stated in the previous section, we refer to the behavior of the kink in these cases as that of a "bare" (long wavelength) or a "renormalized" (short wavelength) particle. It is also important to notice that this result agrees with the perturbative calculation we have just described, as was to be expected. There we showed that the correction to the center of mass motion was basically an oscillatory term, implying that the velocity of the center of mass oscillates around some mean value. This is precisely the same kind of trajectory followed by a point-like particle in the potential in (3.17) (at least if the velocity is not too close to 1).

Nevertheless, to show the power of the collective coordinate approach and, specifically, the advantage one has, in this version of the technique, in knowing about single particle behavior on a potential, it is worth pursuing this agreement a little further by studying the threshold for kinks to propagate in this kind of potential. The easiest way to compute the threshold is by equating the kinetic energy of the kink to the maximum of the effective potential, provided we restrict ourselves to the nonrelativistic limit (v^2 not too close to 1) to keep the kink mass constant. This will give us the maximum potential height over which a kink that starts from a point at which the perturbation is zero with a certain velocity is able to pass the nearest top point. Using the fact that the mass of a not too fast kink is 8 in our units, we find that the threshold is given by

$$\epsilon_{\text{thr}} = \frac{2v^2\gamma^2}{k\pi} \sinh \frac{k\pi}{2\gamma}. \tag{3.18}$$

In the same way, we could have computed the threshold velocity for a given strength of the potential, but we prefer to check our predictions this way because the presence of γ makes the other possibility more complicated. We compared this prediction to numerical simulations. We show an example of this comparison in Fig. 3.3, where we study the propagation of a kink with initial velocity 0.2 (i.e., in a nonrelativistic situation) on a potential of a moderately long wavelength. The predicted threshold for kink propagation as given by (3.18) is $\epsilon_{\text{thr}} = 0.0424$; from Fig. 3.3 we see that the numerical result is bounded by $0.043 < \epsilon_{\text{thr}} < 0.0435$, meaning that the error in our prediction is at most of 2% which is quite satisfactory. We have checked several other cases [52], and an excellent agreement is always found, even for rather large values of the perturbation potential.

The preceding discussion relates to one kind of trapping phenomenon, easily understandable within the collective coordinate picture. We now conclude this section

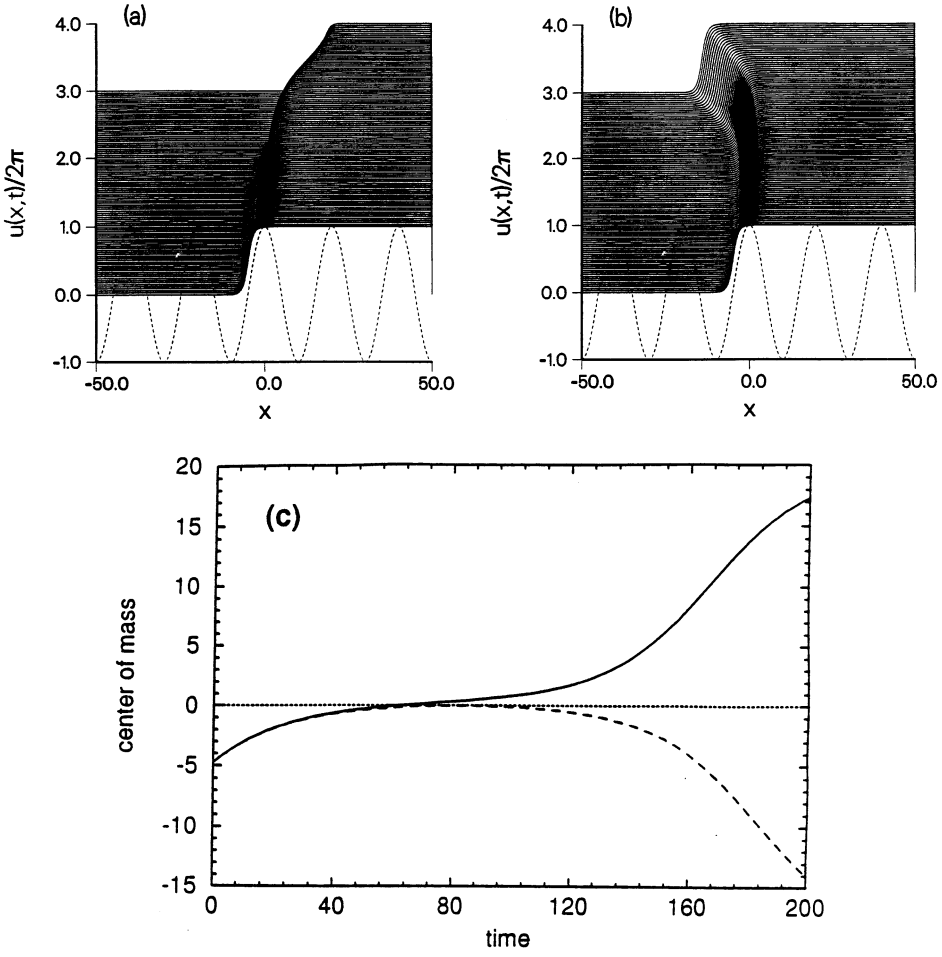

FIG. 3.3. *An example of the verification of the collective coordinate approach predictions. For a kink starting from a midpoint of a potential of wavelength* 20, *with velocity* 0.2, *the predicted threshold for propagation is* $\epsilon_{\text{thr}} = 0.0424$. (a) $\epsilon = 0.43$ *and the kink propagates;* (b) $\epsilon = 0.435$ *and the kink is reflected by the potential maximum;* (c) *center of mass motion for better comparison of both cases; solid line corresponds to the simulation in* (a) *and dashed line to that in* (b). *Final time is* $t = 200$. *Notice the complete absence of radiation in this phenomenon.*

on the collective coordinate treatment of the problem by discussing another unexpected prediction of it that it is numerically verified, relativistic effects playing now the relevant part. This is indeed the second kind of trapping advanced in section 3.1.1. By looking again at (3.17), it can be realized that the presence of γ in the potential may give rise to singularities in the neighborhood of the maximum velocity, $v = 1$. To check whether this is so, we integrated numerically the ODE obtained from applying Newton's second law to V_{eff}, and found that if the initial conditions were those of a particle starting at the top of a large potential, the velocity of that particle would grow as it slides down the potential; of course, if the potential is large enough, the velocity can reach $v = 1$: In those cases the numerical integration of the ODE broke down. The question then arises whether this is an artifact of our collective coordinate approach or if there is a related phenomenon in the full PDE. We actually found that this ODE prediction is verified, as we show in Fig. 3.4. In this simulation, the initial

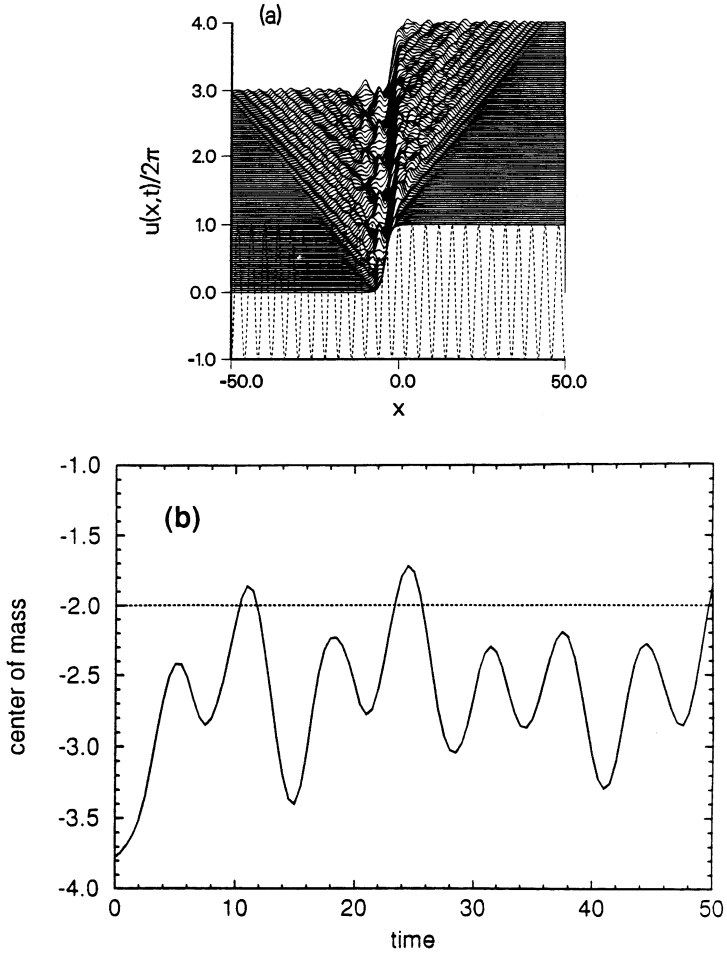

FIG. 3.4. *Trapping of a kink at an intermediate position in the potential instead of at the bottom.* $\epsilon = 2$ *and the kink starts with velocity* 0.1. *The amount of emitted radiation is large due to the fast acceleration of the kink in this large perturbation.* (a) *time evolution of the kink;* (b) *time evolution of the center of mass. The neighboring minimum is at* $x = -2.0$ *(indicated by the dashed line), and the kink oscillates around approximately* $x = -2.5$. *Final time is* $t = 50$.

condition was a kink at a maximum of the potential with initial velocity 0.1 so as to start its motion from the stable point. As it moves to the nearest well, it accelerates and, eventually, its velocity becomes very close to 1, implying that the kink cannot accelerate further. Then it is trapped at an intermediate point of the potential, instead of continuing its motion to the bottom and losing its energy through radiation. The existence of this counterintuitive phenomenon shows in a very dramatic way the value of a simple approach like the collective coordinate formalism to guide understanding of complicated nonlinear phenomena.

3.3. Length-scale competition.

3.3.1. Numerical experiments. The numerical and analytical calculations described so far allowed us to achieve a quite good understanding of the periodically perturbed sG problem, at least of the basic phenomenology. With that background in mind, we turned to the main motivation for the work [52], namely, to study kink

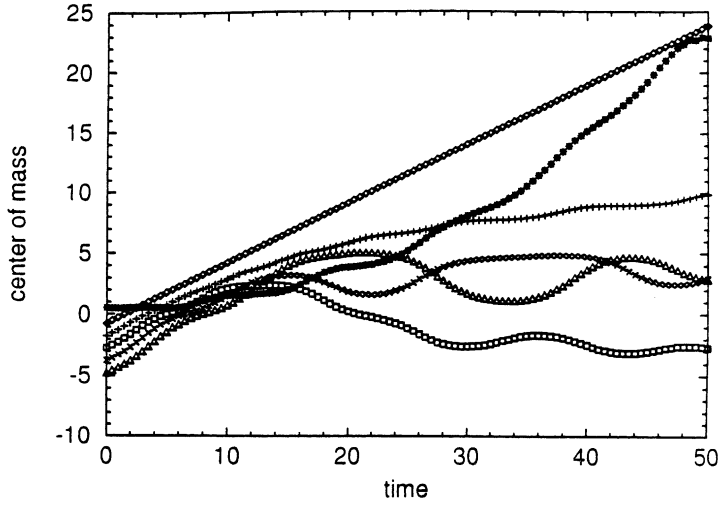

FIG. 3.5. *Length-scale competition. Center of mass evolution of a kink on potentials of different wavelengths, always with* $\epsilon = 0.7$ *and initial velocity* 0.5. *Wavelengths are:* $\diamond$, 1; $+$, 2; $\square$, 3; $\times$, 4; $\triangle$, 5; *and* $*$, 6. *See text for explanation.*

propagation in periodic potential as a step towards the much more complicated problem of breather propagation on periodic media, where we had originally observed the phenomenon of length-scale competition [53] (to be summarized in Appendix B). In principle, we did not expect length-scale competition, whose characteristics will be described below, to arise in this problem, as kinks (because of their topological nature) are very robust objects (which is further confirmed by our above results, in particular by the success of the collective coordinate approach) but we believed that some useful pieces of information may arise due to the simplicity of kinks as compared to breathers. Hence, our purpose was to perform some simulations in the large perturbation regime to see whether any light could be shed on the related breather problem. On the other hand, contrary to the case of the breather, kink widths do not vary much when changing the only parameter governing them, the kink velocity. Of course, when approaching the maximum velocity, Lorentz contraction of the kinks will make them vanishingly small, but that is a regime in which it is very difficult and time consuming to carry out good numerical simulations, so we did not address the problem in that limit. Therefore, the kinks we will be dealing with will have a width of about 6 in our dimensionless units.

The numerical experiments we made were as follows. We studied several potentials of different wavelengths, ranging from 0.5 to 20, i.e., from much smaller than the kink width to roughly three times its width. The initial condition was always a kink at one top of the potential; different velocities were considered. A summary of these experiments in the most interesting range of potential wavelengths is shown in Figs. 3.5 and 3.6. Figure 3.5 shows the motion of the center of mass of the kink on different potentials. The motion in the small or large wavelength limits has been already discussed and it is again seen here. However, a more interesting phenomenon is also evident, namely kink trapping [or even reflection in the case of wavelength 3, see Fig. 3.6(b)]; this trapping was not to be expected because kinks start from a maximum of the potential and with a large initial velocity (in Fig. 3.5, it was 0.5). Regarding this point, we have to stress here that this trapping is of a different kind than the one discussed in the preceding section, which was clearly a nonradiative process. Besides,

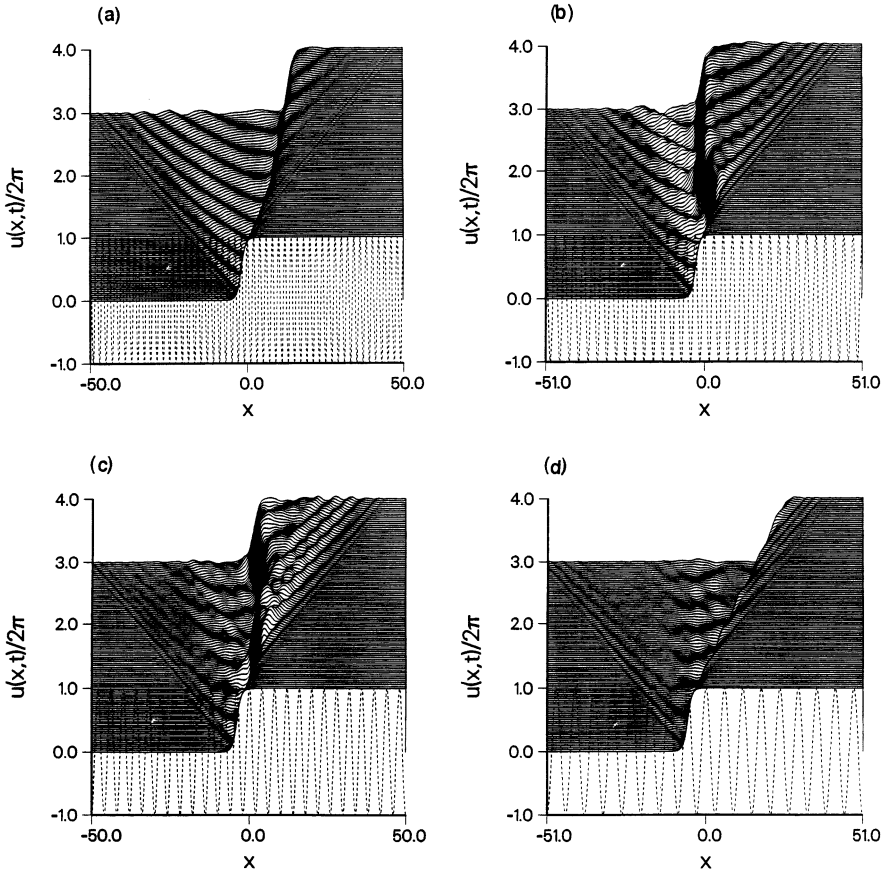

FIG. 3.6. *Time evolution for some of the kinks in Fig.* 3.5. *Wavelengths are* (a) 2; (b) 3; (c) 4; *and* (d) 6. *Notice the different kind of radiation emitted in each case. Notice also that the kink in* (b) *goes back over one maximum of the potential probably due to resonant interaction with radiation left behind. Final time is* $t = 50$.

the trapping depends crucially on the wavelength of the potential. Thus, for instance, in the case of wavelength 2 (Fig. 3.6(a)), the kink is able to propagate over six wells, whereas when the wavelength was 4 or 5 (Figs. 3.6(c), (d)), it was trapped already on the second well. This kind of violent behavior, i.e., of instability, is what we called length-scale competition, the main signature of the role of lengths in its onset being the phenomenon's dependence on the wavelength of the potential. This was further supported by our previous work for the breather case [53], which showed that this competition was most effective when the wavelength of the perturbation was around half the breather width or slightly larger (see Appendix B). This is also the case in these simulations. Another common feature between the problems is that the outcome of a simulation depends very sensitively on the initial condition. This can be understood from the reflection case in Fig. 3.6(b): For the kink to jump back over one potential wavelength it is necessary that it meet the radiation it left behind in the appropriate phase to gain energy from it, and this evidently depends crucially on the initial velocity, as we checked in our simulations. Hence, we concluded that these phenomena are a manifestation of length-scale competition, which we then set out to study in detail, as we now explain.

3.3.2. Linear stability analysis and discussion. The numerical findings we have described in the preceding subsection are of great importance: The existence of processes governed by length-scale competition in the sG kink case opens the possibility of a deeper study of the mechanisms through which this competition affects kink evolution. The relevance of this comes from the fact that, when studying the sG breather problem [53], we were not able to carry out this deeper analysis due to the more complicated nature of the breathers, namely their intrinsic internal dynamics which substantially complicate linear stability analysis [2, 37]. But after finding that this competition also affects kinks, we can certainly study their linear stability analysis, and obtain for the first time an understanding of the mechanisms underlying length-scale competition.

We tested the stability of the analytical continuum solutions as well as of the numerical solutions in the following way. Let the solution to discretization of the sG equation (3.1) be $u_i = u_i^{(0)} + v_i$, where $u_i^{(0)}$ is either the discretized version of the continuum kink or the true minimum energy static solution of the perturbed sG equation (3.1) obtained numerically, and where v_i is a small discrete-valued function whose time dependence is given by $\sin(\omega t)$; the index i runs over the N points of the discrete lattice. The discrete version of the perturbed problem (3.1) is given by

$$\ddot{u_i} - a^{-2}(u_{i+1} - 2u_i + u_{i-1}) + [1 + \epsilon\cos(kai)]\, u_i = 0, \tag{3.19}$$

where a is the lattice spacing. Substituting the proposed form for u_i in (3.19) and linearizing we get

$$\mathbf{\Omega v} = \omega^2 \mathbf{v}, \tag{3.20}$$

where $\mathbf{v}$ is the vector containing the v_i, $i = 1, \ldots, N$, and $\mathbf{\Omega}$ is an $N \times N$ matrix given by

$$\mathbf{\Omega}_{ij} = \begin{cases} 2 + [1 + \epsilon\cos(kai)]\cos\left(u_i^{(0)}\right) & \text{if } i = j, \\ -1 & \text{if } i = j \pm 1, \\ 0 & \text{otherwise.} \end{cases} \tag{3.21}$$

In this formulation, the modes for the linear excitations around the shape $u^{(0)}$ are obtained simply by solving for the eigenvalues ω^2 of the matrix $\mathbf{\Omega}$. We did this for all the wavelengths we were studying, taking for $u^{(0)}$ the exact continuum sG kink at the top or at the bottom of the potential, as well as the numerically obtained solutions at similar positions. The results for our numerical linear stability analysis are shown in Fig. 3.7 for some of the relevant wavelengths.[3]

There are a number of interesting features which deserve comment. First, let us consider the spectra for the exact continuum shapes. When placed at the top of the potential, this gives rise to a negative lowest eigenvalue ω^2, indicating that this continuum kink is not an exact solution of the discrete problem and tends to relax to the correct one by emitting a burst of radiation. The shape at the bottom of the potential does not show this negative eigenvalue but, instead, a single bound state with frequency $\omega^2 \approx 0.3$. This corresponds to a shape mode (i.e., an oscillation of

[3]It is possible to analyze the long wavelength limit of the spectrum analytically, by means of an averaging technique, which leads to the result that the minimum frequency is given by $\omega^2_{min} = 1 - (\epsilon^2/2k^2)$, in good agreement with our numerical calculation of the spectrum as can be seen from the figures.

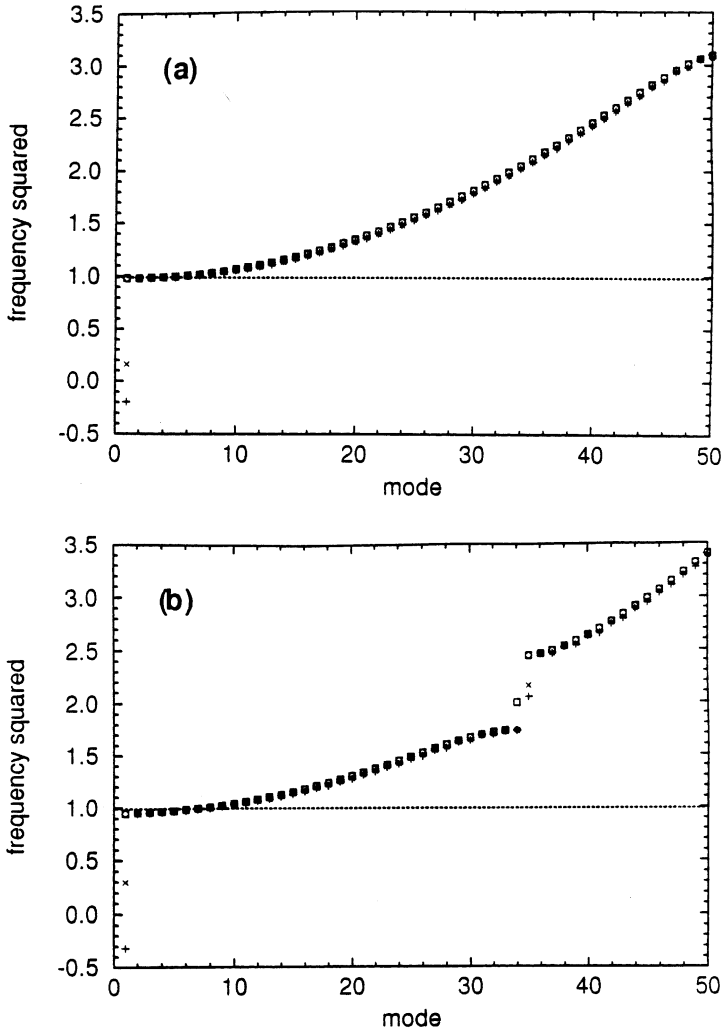

FIG. 3.7. *Frequency spectra for kinks on periodic potentials. See text for details on how it is computed. Spectra for numerical shapes are plotted with* ◇ *(potential maximum), and* □ *(potential minimum). Spectra for analytical shapes are plotted with* + *(potential maximum) and* × *(potential minimum). Wavelengths are* (a) 2; (b) 3; (c) 4; *and* (d) 6. *Notice in this last case that all the first branch of spectrum is below the phonon band.*

the kink profile), similar to that present in unperturbed ϕ^4 kinks, and it actually shows up in simulations: Initial data placed in a potential well (an exact continuum kink) exhibit a static center of mass but a general oscillating shape. This is easily understood if one realizes that in this range of potential wavelengths, different parts of the kink undergo the influence of very different perturbation values (which can be even positive or negative contributions). In response to these gradients, the continuum kink oscillates. These isolated states characteristic of the continuum kinks disappear when we analyze static numerical solutions. It is seen from Fig. 3.7 that in that situation spectra are composed of bands. Actually, this is a common feature for all analyzed shapes, including the continuum ones, and it could be expected from the following argument: Far from the kink center, which only spans a small fraction of the lattice

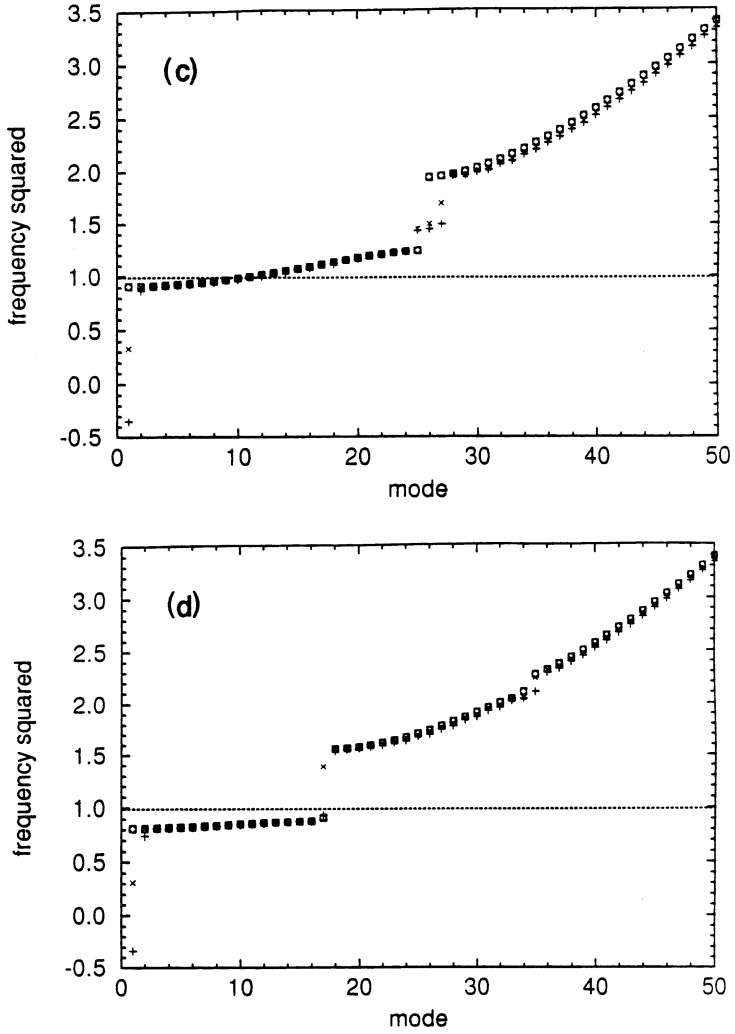

FIG. 3.7. *Cont.*

sites, the nonlinear contribution to the linearized discrete problem for v_i vanishes, and one is left with what is a standard Floquet (Bloch) problem. The corresponding structure is very well known, and in fact it is very much like the ones we show here, with gaps at positions that depend on the potential wavenumber and gap amplitudes that depend on the potential strength.

By comparing the spectral structure we have obtained to the outcome of the numerical simulations, especially to the radiation emission (Fig. 3.6), the mechanism for kink destabilization can be inferred. In the case of small wavelength potentials, the spectrum is very similar to the unperturbed sG one (see Fig. 3.7(a)). In fact, when the wavelength is very small, the height of the effective potential experienced by the kink is so small (due to the sinh term in (3.17)) that this effect is hardly noticeable (hence the near-perfect constant motion of the kink on the smallest wavelength potential in Fig. 3.5). As the wavelength increases, more and more modes move below the phonon band, inducing shape oscillations of the kink, and as a consequence of this motion,

long wavelength radiation is emitted (clearly seen in Figs. 3.6(a) and (b)). This is possible because in those cases there is still a large number of available modes just above the phonon band. Note that the lower limit of the phonon band is given by $\omega = 1$; lower frequencies are localized, because they cannot propagate in the system far from the kink, where the spectrum structure is essentially the unperturbed one. This combined effect induces a rapid destabilization of the kink and its trapping. Finally, if the wavelength is further increased, all the first band eventually moves below the phonon band (Fig. 3.7(d)), and hence long-wavelength emission is strongly suppressed (Fig. 3.6(d)), which stabilizes the kink, making possible its propagation. The effect of the shape modes coming from the first band is still revealed by the kink shape oscillations (see Fig. 3.6(d)). We believe that this interpretation clearly explains the mechanisms leading to the appearance of length-scale competition in sG kinks. To confirm this, we located the approximate value of the potential wavelength at which the last mode in the first band crosses the phonon band, and found that this happens for a potential wavelength between 5.2 and 5.3. Were our hypothesis true, kinks would not be able to propagate on the former potential and they would be able to do so on the latter one. Numerical simulations confirmed that this is indeed the case. Interestingly, the radiation is quite different in both cases and, furthermore, for the trapped kink trapping occurs at the second potential well, indicating that the small number of modes available to radiate prevents a very rapid decay of the kink. We thus conclude that our interpretation is indeed correct. As a matter of fact, as this feature of the spectrum will also be present when considering breather propagation (recall that the reason for the appearance of the gaps is the perturbing potential acting on the wings of the excitation, and the nature of the center becomes less relevant), our explanation of length-scale competition should also apply to the phenomena experienced by breathers, which we will summarize in Appendix B.

3.4. Recent developments.

3.4.1. Recent collective coordinate results. Very recently, Willis [64] has revisited the problem of the periodically perturbed sG equation (3.1) by means of the collective coordinate approach developed by himself and Boesch [9]. The starting point is the ansatz

$$u(x,t) = \sigma[\Gamma(t)(x - X(t)] + \chi[\Gamma(t)(x - X(t), t], \tag{3.22}$$

where $X(t)$ represents of course the kink position and $\Gamma(t)$ represents its slope. It is interesting to point out here that the function $\Gamma(t)$ is a somewhat different kind of collective coordinate in the sense that, whereas the expression with $X(t)$ is a solution of the unperturbed equation, the one with $\Gamma(t)$ is not unless $\Gamma(t) \equiv (1 - X^2)^{(-1/2)}$; therefore, $\Gamma(t)$ has often been called a "parametric" collective coordinate. Whatever the case, for a nonrelativistic, $\dot{X} \ll 1$, treatment, in [64], the above choice for Γ is made and no equation for its evolution is needed, simplifying the treatment while retaining its main features. The equation for $X(t)$ is obtained by substituting (3.22) in (3.1), multiplying by σ', and integrating over x, yielding again a pendulum equation for X (essentially the same that arises from the effective potential (3.17)). However, the inclusion of the phonon term χ makes transparent the main conclusion arrived at in section 3.1.3, namely that there is no radiative divergence because in this approach it can be shown that the energy gained by radiation is lost by the kink. Note also that this implies that the kink velocity cannot be constant, in agreement with our previous discussion. This treatment also explains the small radiation we observed both above

and below the threshold as anharmonic waves, and predicts finite amplitude harmonic radiation (phonons) above the threshold, which should be clearly observed for large kink velocities (not studied in [52]).

In our opinion, however, the important new conclusion drawn in [64] is by far that the periodically perturbed sG equation is connected to the unperturbed, but discrete in space, sG equation. It is well known (see, e.g., [45, 65] and references therein) that discretization, by breaking the continuum translation symmetry, induces an energy barrier (the so called Peierls-Nabarro barrier) to the soliton motion, which in turn gives rise to a periodic potential with period given by the discretization mesh size. Therefore, it is natural to think that the periodically perturbed sG equation must be related to the discrete sG one. The work [64] shows nicely how the qualitative behavior of the continuum $\cos kx$ perturbed system is a special case of the phenomena that occur at the lower band edge in the discrete sG problem, the connection arising because the equation for the collective coordinate in the continuum case is indeed a restriction of that for the discrete problem. This result illustrates once again the power of collective coordinate ideas, in this case to connect rigorously problems that are in principle very far from each other.

3.4.2. Forced periodically perturbed sG equation. Although they are studies of a slightly different problem, let us mention that in recent works [18, 19] the forced propagation of sG kinks on a periodic potential has been studied. In the first one [19], the question addressed is that of soliton propagation in the presence of weak damping and driven by an ac force. A relativistic equation for the kink center chosen as collective coordinate is derived by means of conserved quantities. In this case, the equation is a complicated ODE which cannot be treated in an exact manner, and therefore numerical simulations of the full PDE are compared to numerical integration of the collective coordinate ODE. The main result of the perturbative treatment, confirmed by the PDE simulations, is that the ac force can induce a dc motion of the soliton at a resonant velocity determined by the driving frequency and the period of the perturbation, provided the driving amplitude exceeds a critical value. Whereas at relativistic velocities these "phase-locked" solutions are easily found in the PDE, at nonrelativistic velocities the basin of attraction, in position-velocity space, for them becomes smaller; therefore, although such solutions exist, they are difficult to obtain numerically. The collective coordinate equation is analytically treated in the relativistic limit and found to be in good agreement with the simulation results. Finally, the work reported in [18] elaborates on the previous study by adding a simultaneous dc force to the equation, showing that a similar phenomenology arises and computing the $I - V$ properties of the Josephson junction modeled by such an equation for the purpose of comparison with real experiments.

4. Discussion and conclusions.

4.1. On collective coordinate perturbative theories. In this review, we have illustrated a number of techniques which are pertinent to perturbed soliton-bearing equations, ranging from those based on the inverse scattering transform to direct perturbative expansions, discussing some of them or referring to original sources. Although most approaches mentioned are capable of describing different types of behavior found in these and related equations and are therefore valuable, we particularly want to highlight the versatility, wide applicability, and ease of use of the collective coordinate formalism, which stands as the first choice to deal successfully with many soliton-bearing PDEs. Comments in the preceding text as well as Appendix A support

this claim. Some remarks are in order here. First, collective coordinates as we have discussed them are a very fruitful tool to understand spatiotemporal chaos in nonlinear PDEs. For instance, in [55] a collective coordinate approximation is used to map the periodically perturbed NLS equation to a nonintegrable particle dynamics with an effective Hamiltonian which serves to analyze the original PDE chaotic dynamics; the approach is rather general and applies to many other perturbed problems for solitons. Second, even if the PDE of interest has no soliton solutions, the idea of the collective coordinate technique can still be applied in a generalized sense. This is the case, e.g., with recent work [13] where spatiotemporal chaos in the Kuramoto–Sivashinsky equation is studied by means of a hydrodynamic theory for defect evolution, obtained from a careful examination of the local dynamics of cellular solutions. As a result, a stability mechanism is identified in terms of the interactions of these defects, which, in essence, play the role of solitons (viewed as "particles"). In fact, a model of interacting classical particles on a line has subsequently been developed to represent Kuramoto–Sivashinsky dynamics [50], showing the benefits one can take from this particle picture. Third, collective coordinate techniques are by no means limited to one spatial dimension; indeed, they are even more important in two or more dimensions as the calculations required for other perturbative approaches in such problems become very cumbersome upon increasing the number of spatial variables. As an example, in [39] very good results have been obtained by using this approach to study the motion of vortices in two-dimensional easy-plane ferromagnets, described by the Landau–Lifshitz equation. In fact, this work is also relevant as for the first time it suggests a rather systematic procedure to improve the approximation of this kind of calculation by obtaining higher order ODEs. Interestingly, for this particular problem it is shown that to capture the whole phenomenology of the problem it is necessary to resort to the fourth-order equation. Finally, we want to mention that if the coherent structures on which the collective coordinate technique rests do exist, they can be identified and their independent features understood by means of a method developed in [42], thus widening the range of applicability of this robust perturbative approach.

An aspect which deserves emphasis is the necessity of feedback between any perturbative approach and computer simulations. The reader has probably realized by now that without simulations we would still believe older perturbative results for the periodically perturbed sG equation, which we have shown to produce a very misleading picture of its solutions. Moreover, simulations not only served to falsify those perturbative calculations, but also provided hints as to the correct approach to the problem, i.e., they do not simply play a negative role but rather can be also used in a constructive manner. As Zabusky [66] put it, "... by the *judicious* use of computers, we can penetrate into new areas and discover linkages to diverse areas of mathematics unforeseen by our forebears." These notions are of course not new; however, the input from analytics into computer work mentioned in the previous paragraph is of a newer character, and we envisage that the combination of cellular automata algorithms to simulate PDEs with collective coordinate ideas for describing the particle-like dynamics of the coherent entities in the equation can pave the way to large-scale simulation procedures for the complicated PDEs arising in problems such as turbulence, plasma dynamics, or oceanography.

Clearly, much work remains regarding the foundations of collective coordinate techniques. An important point still to be clarified is the relationship between the plethora of procedures now available to carry out such a nonlinear reduction. Different approaches lead to slightly different results for the same problem, and it is a

matter of practice by now to decide what is the best one to address a specific problem. So far, the most rigorous interpretation of this technique is as a zeroth-order term in perturbative expansions [9, 21, 38], but this expansion is problem dependent and therefore not always available or tractable for the problem at hand. It is therefore necessary to pursue a rigorous mathematical framework which permits the use of a collective coordinate approximation in a controlled manner; we believe that, if formulated in principle for soliton-bearing equations, it could subsequently be generalized to a much wider class of nonlinear PDE's following some of the ideas mentioned in the previous paragraph.

4.2. On length-scale competition. In addition to our discussion of perturbative techniques, we have presented a case study of an example of the phenomenology arising in soliton-bearing equations when several length scales compete and drive the system towards or between asymptotic states (space-time attractors). We hope that the case we have summarized plus those contained in Appendix B will be sufficient to substantiate that such length-scale competition is a key to the study of very many nonlinear inhomogeneous systems as well as of their governing partial differential equations. Thus, identification of the relevant length scales provides a correct qualitative picture of the corresponding bifurcation diagram of the problem, which usually consists of a (small) parameter region exhibiting complex (chaotic) behavior clearly different from other regions, each one of them defined by the dominance of one of the scales involved in the problem. The sG example in section 3 (for kinks) and Appendix B (for breathers) is an instance where the scales are evident from the posing of the problem; the NLS equation in Appendix B will show how the competing scales can arise dynamically. Whatever the source of competition, it becomes apparent that this is a rather general phenomenon and, as such, we believe that it is an important and useful paradigm that must be kept in mind in order to understand space-time complexity (including intermittency and chaos) in (particularly, but not exclusively, soliton-bearing) nonlinear PDEs, a subject whose general features are not very well delineated at present.

An important open question, where applied mathematicians can certainly contribute, relates to this phenomenon of length-scale competition. Let us recall that we have found a physical explanation of the mechanism behind the complex behavior of one specific system, but it is naive to think that this line of reasoning can be applied to all instances where length scales compete, because those scales can arise through very different mechanisms as we have noted. Also, usual perturbative expansions break down in this regime: as we have shown in this paper, these are nonperturbative phenomena even if the perturbation is small; collective coordinates are no longer useful in their present form because new excitations appear, and the original solutions are too much distorted from the basis around which one would expand to obtain the solution to the perturbed problem. It is clear that finding a way to analyze PDE's in this parameter region is a complicated task, but we hope that the paradigm of length-scale competition can be of help in providing clues to correct analytical approaches.

4.3. Outlook: Nonlinearity with disorder. The work reported here relates to soliton behavior on spatially periodic potentials. In studying this kind of problem, one of our motivations has been the necessity to understand previous perturbative results for the sG equation. Another reason to study this problem is certainly its applicability: These kinds of problems are interesting in their own right, e.g., because of modern nanotechnology patterning techniques in electronics or optics, such as those

employed in building Josephson devices [23]. However, there is a third goal in pursuing this research, namely, to understand periodic perturbations as a fundamental step in order to proceed with the more complicated case of nonperiodic or stochastic perturbations, i.e., *disorder*. In spite of the enormous progress both in understanding the effects of disorder in linear problems and in dealing with nonlinear PDEs, the available knowledge on nonlinear, disordered systems is still very limited, even though a lot of work in this direction has recently been carried out [7]. Both nonlinearity and disorder may give rise to (self-)localized excitations; therefore, it is natural to ask whether these effects reinforce, complement, or frustrate each other. Transport properties in these systems will depend strongly on whether solitons behave as particles (the way we have been describing) in the presence of disorder or interact very strongly with other degrees of freedom. Does the nonlinearity lead to adaptive behavior of excitations in disordered systems which preserve coherence? How do nonlinear waves interact with each other in the presence of disorder? Does initially distributed energy self-focus as in modulationally unstable nonlinear equations? These and other issues are of great concern in very many fields. In view of them, we addressed the periodic perturbation problem as a case study where we could identify phenomena relevant to the disordered case. The hope is that deterministic aperiodic, or random, potentials can be understood in terms of their Fourier components, the properties of which are those known from the present work. In fact, the results for the NLS equation summarized in Appendix B clearly support this idea. Thus, we believe that the fact that the disorder contains length scales close to those of the typical nonlinear excitations of the problem considered will lead to (a surely more involved) length-scale competition, whereas for the remaining Fourier components a particle description will still hold. We hope that research along this line can shed light on this and related questions.

Appendix A. More examples of collective coordinates. In this appendix, we briefly summarize some other, more elaborate applications of collective coordinates than those discussed so far, thus providing further references for the interested reader as well as pointing out specific procedures we have not mentioned in the body of the manuscript. We conclude with a particular instance where collective coordinates *cannot* be applied, and discuss why is it so and what can be done instead.

Our first example is the application of collective coordinates to a random system: The case of sG kinks propagating along a lattice of delta function impurities. This is considered in [24], where collective coordinate analysis allows us to understand the problem in terms of a particle propagating in randomly placed sech-like potentials. Subsequently, the problem is reformulated in terms of the time domain instead of the spatial domain, by considering the time the soliton needs to travel through one of those potentials at a given velocity (which can of course be exactly computed) and the time elapsed freely propagating between impurities (which is a random variable insofar as the separation between impurities is random). In this representation, asymptotic predictions for the kink evolution (in fact, for any magnitude depending on the kink coordinate) can be obtained quite straightforwardly. In this case, the main virtue of collective coordinates is that they are an intermediate stage in the solution of the problem, useful to pose it in an analytically solvable way.

The second example pertains to the realm of discrete systems, which are receiving much recent attention, mostly since the discovery of intrinsic localized excitations in such systems [58, 61] some 10 years ago. Collective coordinate approaches to discrete systems have been proposed even earlier than that [65], the main ideas of which are the same as for continuum equations, but for which calculations are of course more cumbersome. In the example we propose here, however, our aim is to show that it may

be necessary to go beyond the usual approach in order to obtain the correct result. For this, consider the system of differential equations given by the driven, damped, discrete sG equation

$$\ddot{u}_n - \frac{1}{a^2}(u_{n+1} - 2u_n + u_{n-1}) + V_n \sin u_n + \alpha \dot{u}_n = F.$$

In [14], a perturbation of this problem was considered, again of the potential type, i.e., $V_n = 1 + \epsilon_n$, where ϵ_n takes only two values, ϵ_a and ϵ_b, arranged according to the Fibonacci sequence $ABAAB\ldots$ The driven, damped, continuous sG equation was already studied by means of collective coordinates in [38], and it was shown that a kink, if initially at rest, acquires a velocity given by $v_\infty = \sqrt{1 + (4\alpha/\pi F)^2}$ due to the balance of damping and driving. As noted above, the collective coordinate results can be extended to the discrete case, leading to the similar result that solitons again acquire a definitive velocity given by $v_\infty = \sqrt{1 + V_{avg}(4\alpha/\pi F)^2}$, V_{avg} being the weighted average of ϵ_a and ϵ_b. However, numerical simulations show that, whereas for the discrete sG equation, as above but with $V_n = 1$, the prediction is very approximately fulfilled, for the Fibonacci sG equation a force above a certain threshold is needed to initiate the kink motion, in disagreement with the collective coordinate results. In [14], the problem was traced to the high degree of order of the Fibonacci chain, which breaks translational symmetry in such a way that the value for the effective potential seen by the collective coordinate (the soliton center) depends strongly on the precise lattice site around which one computes it. This difficulty can be solved following the ideas of Salerno and Kivshar [51], who suggested averaging the effective potential over an interval of the lattice. The threshold for the Fibonacci chain is thereby correctly predicted [14] with a very good agreement with the numerical simulations.

The above paragraph shows that even when straightforward collective coordinate approaches fail, it does not mean that the idea of coherent entities is useless in that specific problem. Many times it means that one may have to go further into the details of the problem and the coherent excitations to build a correct collective coordinate treatment. In some cases, the solution to such obstacles can come from choosing different variables as coordinates. For instance, in [30], where an NLS equation with a perturbing lattice of delta-functions was studied, instead of resorting to the traditional choice of the center of the soliton as a function of time as collective coordinate, the energy and the norm of the soliton solution as a function of its spatial position were used as working variables. Such an approach allows one to predict that "sufficiently nonlinear" (meaning basically large norm-to-velocity ratio) solitons readjust themselves to the lattice and propagate along it, whereas "quasi-linear" solitons are annihilated into linear waves. Subsequently, an experimental device was built specifically to check this prediction for surface waves on a fluid (superfluid helium), a system related to the one just described, yielding results in agreement with the existence of such a threshold [26].

Sometimes collective coordinate perturbative approaches do fail. This happens typically (but not always, as the above cases with additive forces applied on the whole real axis show) in problems where the perturbing terms act on the whole system and not only on the solitons or nonlinear excitations of interest. As an example, consider the perturbed ϕ^4 equation

$$u_{tt} - u_{xx} - u + u^3 = h_{10}\cos(\omega t) + u\, h_{20}\cos(\omega t + \phi) - \alpha u_t,$$

which was studied by means of collective coordinates in [60]. Those authors resorted to this technique in spite of the fact that there are two ac forces (the h_{10} and h_{20}

terms) which affect the whole system, not only the ϕ^4 kink. In addition, the action of the h_{20} term is asymmetric; recall that the values of the ϕ^4 kink at infinity are $u(\pm\infty, t) = \pm 1$. The results in [60] predicted that these oscillatory forces induce kink motion with constant velocity in one direction, which is not a surprise in view of this asymmetry; the velocity modulus was predicted to be proportional to ω^{-4}. Suspecting that collective coordinate results would not be accurate for this problem, numerical simulations were carried out in [32], finding that the correct result for the induced velocity is ω^{-2}. This behavior can be easily predicted analytically by means of an averaging technique such as those mentioned in section 2 [32]. This result emphasizes the importance of combining the collective coordinate (or any other type of) perturbation theory with numerical simulations in order to make sure of the accuracy of the analytical predictions, as already stated in the discussion in section 4. In any event, even though we recommend enthusiastically the use of collective coordinate ideas, we do not claim they are universally applicable!

Appendix B. More examples of length-scale competition.

B.1. sG breathers on a periodic potential. Consider again the periodically perturbed sG equation Eq. (3.1). In section 3 above, we have been discussing the problem of sG solitons (or kinks) propagating on this potential. However, as is well known, there is another type of solitonic solution to the sG equation, the so-called breathers, whose name comes from their oscillatory character. At rest, they are given by

$$u_b(x,t) \equiv 4 \tan^{-1}\left(\tan\mu \frac{\sin[(t-t_0)\cos\mu]}{\cosh[(x-x_0)\sin\mu]}\right), \tag{B.1}$$

t_0 being an initial phase and x_0 being its initial position. As stated above, breathers are oscillating excitations (see Fig. B.1(a) for an example) that breathe with frequency $\cos\mu$, with $0 \le \mu \le \pi/2$. Breathers with $\mu \to 0$ are of small amplitude, very similar to linear waves or phonons, whereas when $\mu \to \pi/2$ they become almost static (i.e., they do not oscillate) and can be regarded as a bound state of a kink and an antikink. Whatever the case, each breather has a characteristic width, roughly $\lambda_b \sim 1/\sin\mu$. This will be one of the length scales in the problem, the other one being of course the potential period $\lambda_p = 2\pi/k$.

In [53, 56] the behavior of static breathers was studied analytically and numerically. We note here that, opposite to kinks, which are one-parameter (the velocity) solutions, breathers are two-parameter (velocity plus frequency) solutions. (Expressions for moving breathers can be obtained from (B.1) by an adequate Lorentz transformation.) The existence of two independent parameters makes the problem much more complicated and therefore it was decided to restrict the study to static (zero velocity) breathers with the hope that it would be useful for the more general case (which it indeed is, due to the findings regarding length-scale competition as the key feature of such a problem). Numerical simulations showed that when the initial breather has a length far from that of the potential, it remained unbroken (see Fig. B.1(b) and (d)). By unbroken we mean that it is altered with respect to the initial breather but still retains its coherence and behaves like a single elementary excitation. The main changes it undergoes are a modulation of its shape, which develops "ripples" if $\lambda_b > \lambda_P$ (not visible at the scale in Fig. B.1(d) for this small ϵ value) with the same period of the perturbation potential (i.e., the soliton adapts to the perturbing term as mentioned in the introduction), and an increase of the breathing frequency. In

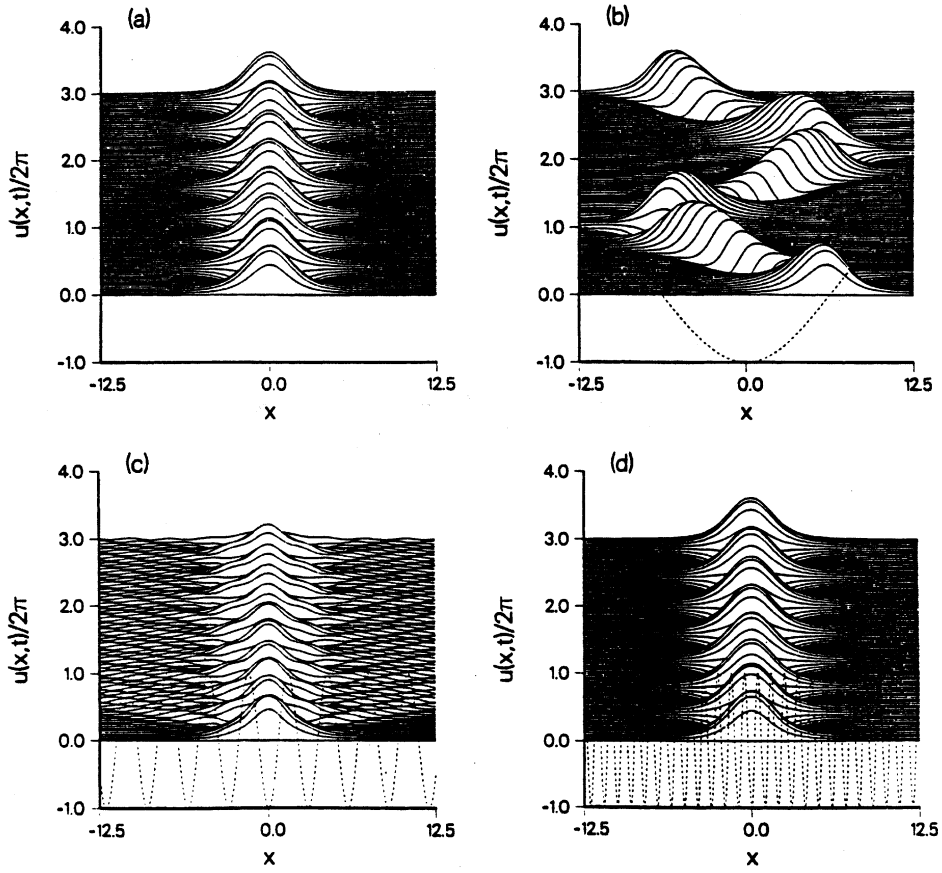

FIG. B.1. *Numerical simulations of breathers for the sG equation* (3.1). *We plot* $u(x,t)$, *time increasing upward. Dashed line sketches the potential, not to scale.* (a) *No potential,* $\epsilon = x_0 = 0$. (b) *Long-wavelength potential* ($\lambda_b << \lambda_P$), $\epsilon = -0.5, k = 2\pi/25, x_0 = 6$. (c) *Breather breakup for competing length scales,* $\epsilon = -0.5, k = 2\pi/3, x_0 = 0$. (d) *Short wavelength potential,* ($\lambda_b >> \lambda_P$), $\epsilon = -0.5, k = 2\pi, x_0 = 0$.

this regime there is a good qualitative agreement with the predictions from the collective coordinate approach [56]: Indeed, when $\lambda_b/\lambda_P \to 0$, the breather behaves very much as a rigid particle (see Fig. B.1(b)), including features such as being eventually removed from its equilibrium position by numerical roundoff errors and then falling down to one of the two neighboring wells. On the other hand, when $\lambda_b/\lambda_P \to \infty$, it can be shown that the effects on the breather, both on its shape, its frequency, and its center position, become barely visible, i.e., using the same terminology as for kinks above, the breather behaves like a renormalized particle; as in the kink case, the potential vanishes exponentially with increasing wavenumber of the perturbation.

This picture changes dramatically as the initial breather approaches the competing lengths region, $\lambda_b \approx \lambda_P$. In this regime, the breather is no longer stable: It emits a large amount of energy in the form of radiation and decays rapidly (see Fig. B.1(c)); if the amplitude of the breather is large enough it can also decay to a kink-antikink pair. Sometimes this takes place spectacularly: The initial breather jumps over several potential wells and finishes by breaking into several breatherlike excitations, hardly distinguishable from radiation. This happens even for tiny values of ϵ; remarkably,

small changes in this parameter can lead, for large amplitude breathers, to breaking into kink-antikink pairs, into other breathers, or into simple radiation. In general, the outcome is very sensitive to the precise ϵ value. This scenario of highly complex behavior is once again length-scale competition. The two lengths present in the system tend to drive it in different ways, leading to a "violent" solution that implies the suppression of one of the scales (in this case, the only possible one, the breather length, as the perturbation and its characteristic length are imposed externally and cannot be removed). As in the kink case, the identification of relevant length scales has yielded a simple interpretation of a quite varied and complex phenomenology. The main difference with kinks is that breathers are intrinsically less robust objects because of their null topological charge, and therefore undergo the bifurcations of length scale competition in a much more clear and destructive way.

B.2. Nonlinear Schrödinger solitons on a periodic potential. As a final example of length-scale competition, we briefly summarize here the quite complete study of the periodically perturbed NLS equation carried out in [54]. The equation under consideration is

$$i\Psi_t + \Psi_x x + 2\Psi|\Psi|^2 = \epsilon\Psi\cos(kx), \tag{B.2}$$

Ψ being a complex quantity. Its unperturbed soliton solution is given by

$$\Psi(x,t) = 2i\eta\frac{\exp[i\dot{q}x - i\Phi(t)]}{\cosh(2\eta[x-q(t)])}, \tag{B.3}$$

where $q(t) = -4\xi t + q_0$ is the soliton position and $\Phi(t) = 4(\xi^2 - \eta^2)t + \Phi_0$ its phase, with ξ and η the parameters that characterize the soliton. The first one, ξ, is basically related to the velocity, whereas the second one, η, is equivalent to the μ of the sG breather solution and controls the amplitude and length of the soliton. Notice that in this second example we consider solitons with any velocity, not only at rest as in the previous section.[4]

We start the discussion of this problem by noting that for static or slowly moving solitons all the comments made above for sG breathers apply directly. The same regime separation due to length scale competition happens: Destabilization when lengths match, particle-like behavior when the potential length is much longer than the soliton one, and renormalized behavior in the opposite limit. There are no new phenomena here. Nevertheless, there is something worth mentioning. In [54], it was checked that the effects of sufficiently different wavelengths on a soliton were felt by it separately. This can be seen in Fig. B.2, where a soliton moves on a two-wavelength potential: The large one drives its motion whereas the short one just induces ripples in its shape, implying the above assertion. This checking was required if we are to pursue our goal of interpreting random potentials in terms of Fourier components as discussed in section 4.3. The results shown here support this idea.

Let us now turn to the important new point of this example. If we assume that the solution to the perturbed equation is a soliton plus a modulation with the same length of the potential, which is sensible in view of the simulation outcome, it is easy

[4] The problem with doing the same for the sG equation comes from its Lorentz-invariant nature, that imposes a maximum allowed velocity and all the relativistic phenomena such as length contraction, for instance. This introduces problems that would burden the current discussion with new phenomena.

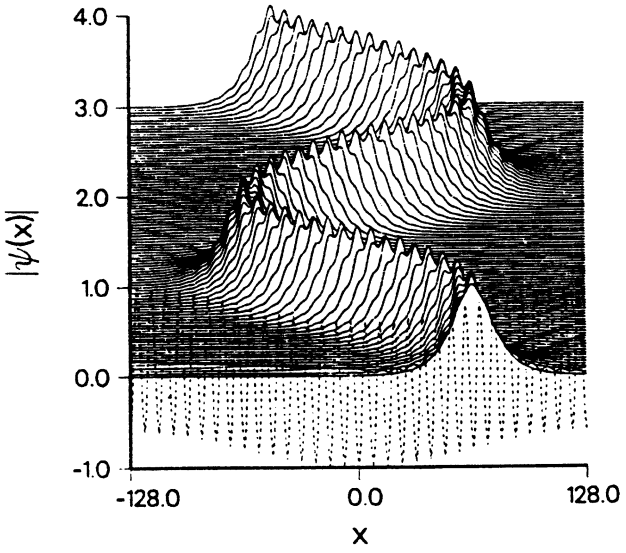

FIG. B.2. *Numerical simulation of a NLS soliton on a potential of the form* $V(x) = \cos(k_1 x) + r\cos(k_2 x)$ *instead of the term* $\cos(kx)$ *in* (B.2). *Here* $32k_1 = k_2 = \pi/4$, *and* $r = 4$. *Notice the different effect each component of the potential has on the soliton motion.*

to show by multiple scale expansions that, to $O(\epsilon)$, such a solution fulfills

$$|\Psi(x,t)|^2 = 4\eta^2 \mathrm{sech}[2\eta(x-q)]\left(1 - \frac{2\epsilon\cos kx}{k^2 - \dot{q}^2}\right). \tag{B.4}$$

What this equation predicts is that if $|\dot{q}| < k$ ($|\dot{q}| > k$) the solution modulation will be out-of-phase (in-phase) with the potential. When $|\dot{q}| = k$, the perturbative result (B.4) suffers from a singularity, which signals the breakdown of the expansion. Numerical simulations were carried out and verified this prediction, as can be seen from Fig. B.3. Now that we are already familiar with length-scale competition, we recognize the phenomenon depicted in this plot as another example of this process, with the same regime separation and the same complex outcome when lengths match: Indeed, at the resonance the soliton breaks up into a standing wave train with $\lambda = k$ that switches back and forth between being out-of-phase and in-phase with the potential. What is this new length? From (B.3) it is seen that $\dot{q}$ is nothing but the modulation of the phase of the soliton. The fact that this characteristic length of the soliton, distinct from its width, plays a part in the system behavior was unexpected. This new competition may be regarded naively as close to that of two oscillators that try to lock when their frequency is close, and evolve separately otherwise. A final remark is in order to stress that this is a dynamical effect, as $\dot{q}$ (same as parameter ξ for an unperturbed soliton) would be zero for a soliton at rest.

Appendix C. Numerical procedures. The numerical work on perturbed sG equations reported here has been carried out by means of two different procedures: An adaptation of the energy-conserving Strauss–Vázquez [59, 6] finite-difference scheme and a fifth-order, adaptive stepsize, Runge–Kutta integration [46, 47] of the temporal discretization of the PDE. The reason for using two different schemes is basically to check that the results are independent of the numerical procedure. This checking (which in our case was fully satisfactory) is indispensable, the more so if we are going

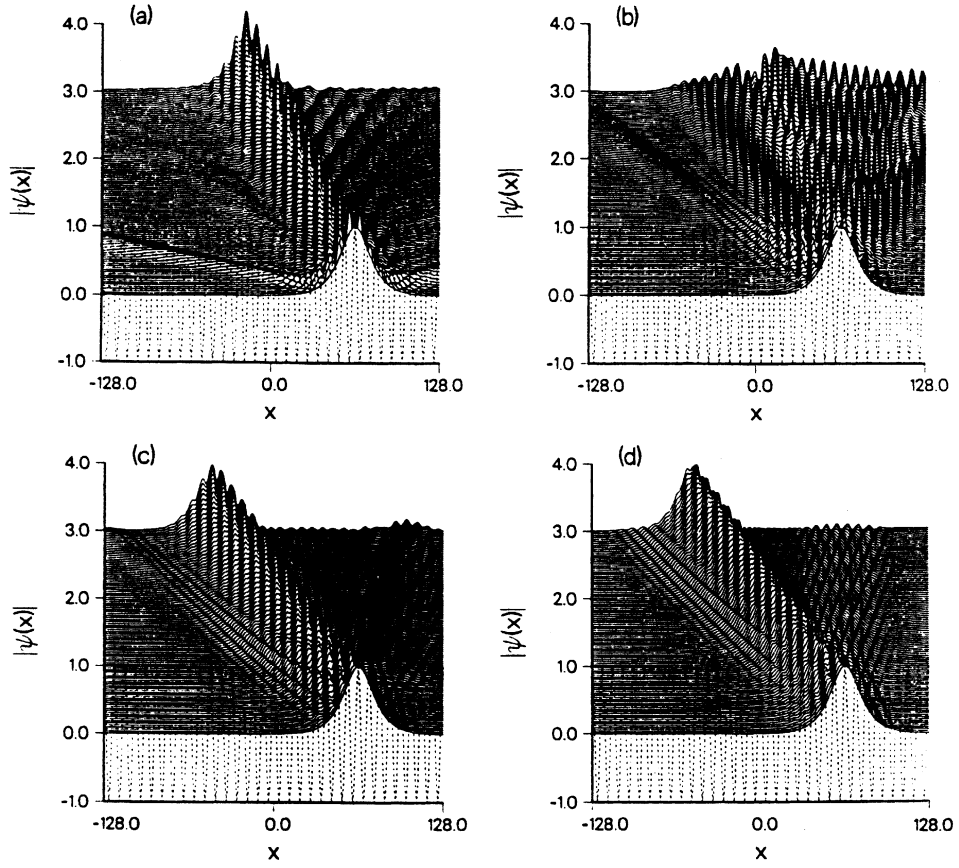

FIG. B.3. *Numerical simulation of NLS solitons showing the phase length resonance. In all four plots,* $\epsilon = 0.1$, $k = \pi/4$, *and* $\eta = 0.05$. (a) $\dot{q} = -0.2$, *integration time* 500. (b) $\dot{q} = -0.8 \approx k$, *integration time* 125. (c) $\dot{q} = -1.2$, *integration time* 100. (d) $\dot{q} = -1.6$, *integration time 80. Although it is difficult to see from the picture, soliton ripples are out -of-phase with the potential below the resonance and in-phase above it.*

to use our simulations to falsify analytical perturbative predictions. The Runge–Kutta algorithm is rather well known, and a full description of its main properties (even the source code) can be found in [46, 47], so we will not dwell on it here; we will describe the less familiar finite-difference procedure.

The Strauss–Vázquez finite difference scheme, adapted for integrating (3.1), reads

$$\frac{u_j^{n+1} - 2u_j^n + u_j^{n-1}}{(\Delta t)^2} - \frac{u_{j+1}^n - 2u_j^n + u_{j-1}^n}{(\Delta x)^2} + [1 + \epsilon \cos(kj\Delta t)] \frac{\cos u_j^{n+1} - \cos u_j^{n-1}}{u_j^{n+1} - u_j^{n-1}} = 0,$$

where $u_j^n \equiv u(n\Delta x, j\Delta t)$, Δx and Δt being the spatial and temporal mesh sizes, respectively. The original Strauss–Vázquez scheme for the unperturbed sG equation is recovered by setting $\epsilon = 0$. The characteristic feature of this algorithm is the apparently strange discretization of the $\sin u$ term, which is nothing but a (centered) finite difference representation of $dV(u)/du$, $V(u) = 1 - \cos u$ (recall that the sG equation and all other nonlinear Klein–Gordon (NKG) equations can be written as

$u_t t - u_x x + dV(u)/du = 0$, and correspondingly all of them can be numerically integrated with this same procedure). This unusual choice has the virtue that the scheme conserves *exactly* a discrete analog of the system Hamiltonian. Based on this property, one can rigorously show [6] that the scheme is (globally) stable and convergent if $\Delta t < \Delta x$. As the scheme for the perturbed equation, $\epsilon \neq 0$, is also conservative in the same sense, the stability proof can be extended to cover this generalization with similar results. In addition, the scheme compares quite favorably with others proposed for NKG equations, including symplectic ones, as carefully studied in [27]. So this is a very good choice for a numerical simulation program on NKG equations; indeed, it could be considered optimal were it not for the fact that it is an implicit scheme and a Newton algorithm is needed to compute u_j^{n+1} at each step, degrading the overall performance of the algorithm (although usually very few iterations are needed for the Newton solver).[5]

In our computations, we took advantage of the fact that the scheme is very robust even when using large steps due to its energy-conserving property. Typical choices for the mesh sizes were $\Delta x = 2\Delta t = 0.1$, which we routinely halved to have another check on the accuracy of the results; some of the runs were repeated even once more with $\Delta x = 2\Delta t = 0.01$ as a further verification. As noted above, we also repeated the calculations with the Runge–Kutta code to verify our conclusions, mostly in connection with the search for the existence or not of a threshold for radiation (see section 3.1.2.). The large values of Δx and Δt allowed us to integrate large systems up to very long times, which is very important in order to explore correctly the emission or not of radiation. As a final test on our results, energy conservation by the code was always accurate to all significant figures.[6]

To complete the description of our numerical simulations, we need to specify what the boundary conditions were. Again, using a single set of them is not enough to ensure the validity of the computations, as their influence on the outcome must be checked. In principle, for radiation power estimation, the best recipe is to integrate on a large system (large as compared to the soliton extent; a system $[-L, L]$ with $L \geq 100$ was usually large enough. See [33] for this kind of accurate radiation measurement, to which the energy-conserving scheme turns out again to be crucial) with initial data given by a soliton located at the center and fixed boundary conditions, $u(L,t) = u(-L,t) = 0$. This is easily implemented and produces a fast code, but if radiation is produced, it is reflected at the boundaries, so after the time the phonons first reached the boundaries the results are affected by them. In our case, we did not observe much radiation, so this was not a serious problem. Repeating the simulations with different system sizes helps exclude finite size effects. However, we did use other kinds of boundary conditions, namely, periodic boundary conditions which are obtained by identifying the leftmost and rightmost lattice points, i.e., turning the domain of integration into a closed ring. By doing this, reflections are avoided, but instead radiation leaving the system by its left boundary returns through its right boundary, interacting with the right propagating waves and eventually with the kink

[5]There is an alternative energy-conserving scheme which is fully explicit at the price of including four different times [17]. This implies more calculations; however, as no Newton procedure is needed because the scheme can be solved for u_j^{n+1}, the algorithm is somewhat faster than the S-V scheme. See also [68], [69], and [70] for more recent work on conservative schemes.

[6]After the publication of [64], tying the nonexistence of divergences to the energy conservation, this is of course much more important; nonconservative schemes might in principle exhibit divergences (see [27] for schemes with spurious blowup phenomena).

itself. Hence, once again there is a limiting time for the validity of the results. What we checked was that within this time window the results of the numerical calculations coincide. Finally, sometimes we also used absorbing boundary conditions. This is the most rigorous way to deal with reflected phonons, although it has the drawback that the code is somewhat slower. In this case, one adds a term $-\alpha(x)u_t$ to the right-hand side of (3.1), i.e., a space-dependent dissipative term. The system size is again chosen to be large, and then $\alpha(x)$ is taken to be zero in the interval $[-0.9L, 0.9L]$ and, e.g., exponentially growing in the remainder of the integration interval, namely, $\alpha(x) = \exp[\alpha_0(x \pm 0.9L)$ (the plus or minus sign corresponding to the left or right sides, respectively) and $\alpha_0 \geq 1$, often taken to be 10, which is a very large value. By doing this, the radiation arriving at the outer parts of the integration intervals is damped out, and the continuity at the transition between the undamped and damped parts ensures that no reflections are produced. By this procedure, the computations remain valid for a much longer time, namely until the soliton itself reaches the absorbing zones. Comparing the results coming from all three sets of boundary conditions, we can be sure that what we are seeing in the simulations does not depend on the boundaries.[7]

Acknowledgments. We are very much indebted to our collaborators in this project for their help in obtaining most of the results and the global picture we have discussed here: Rainer Scharf, David Cai, Francisco Domínguez-Adame, and Yuri S. Kivshar, as well as to Luis Vázquez and Peter Lomdahl, with whom we also worked at various stages of the project. We have also benefited from discussion on these topics with Franz Mertens, Mario Floría, Fernando Falo, and Niurka R. Quintero, who is lately continuing this line of research. A. S. thanks the warm hospitality of CNLS and T-11 at Los Alamos National Laboratory, without which this work would not have been possible.

REFERENCES

[1] M. J. Ablowitz and H. Segur, *Solitons and the Inverse Scattering Transform*, SIAM, Philadelphia, PA, 1981.

[2] S. Aubry, *Breathers in nonlinear lattices: Existence, linear stability and quantization*, Phys. D, 103 (1997), pp. 199–219.

[3] D. J. Bergman, E. Ben-Jacob, Y. Imry, and K. Maki, *Sine-Gordon solitons: Particles obeying relativistic dynamics*, Phys. Rev. A, 27 (1983), pp. 3345–3348.

[4] F. G. Bass, Yu. S. Kivshar, V. V. Konotop, and Yu. A. Sinitsyn, *Dynamics of solitons under random perturbations*, Phys. Rep., 157 (1988), pp. 63–181.

[5] A. Barone and G. Paternó, *Physics and Applications of the Josephson Effect*, Wiley, New York, 1982.

[6] G. Ben-Yu, P. J. Pascual, M. J. Rodríguez, and L. Vázquez, *Numerical solution of the sine-Gordon equation*, Appl. Math. Comput., 18 (1986), pp. 1–14.

[7] A. R. Bishop, D. K. Campbell, and St. Pnevmatikos, eds., *Disorder and nonlinearity*, Springer-Verlag, Berlin, 1989; F. Kh. Abdullaev, A. R. Bishop, and St. Pnevmatikos, eds., *Nonlinearity with disorder*, Springer-Verlag, Berlin, 1992; A. R. Bishop, S. Jiménez, and L. Vázquez, eds., *Fluctuation Phenomena: Disorder and Nonlinearity*, World Scientific, Singapore, 1995.

[8] A. R. Bishop, J. A. Krumhansl, and S. E. Trullinger, *Solitons in condensed matter: A paradigm*, Phys. D, 1 (1980), pp. 1–44.

[7] Let us just mention that one can even choose moving absorbing boundary conditions, which damp away radiation beyond a certain radius around the propagating kink, no matter what its position, see [54]. Whereas the validity time of such a simulation is virtually infinite, the computing time increases substantially, which frequently renders this choice somewhat unpractical.

[9] R. Boesch and C. R. Willis, *Existence of an internal quasimode for a sine-Gordon soliton*, Phys. Rev. B, 42 (1990), pp. 2290–3206.

[10] D. K. Campbell, J. F. Schonfeld, and C. A. Wingate, *Resonance structure in kink-antikink interactions in ϕ^4 theory*, Phys. D, 9 (1983), pp. 1–32.

[11] D. K. Campbell and M. Peyrard, *Solitary wave collisions revisited*, Phys. D, 18 (1986), pp. 47–53.

[12] J. G. Caputo, N. Flytzanis, and C.N. Ragiadakos, *Removal of singularities in the collective coordinate description of localised solutions of Klein-Gordon models*, J. Phys. Soc. Jpn., 63 (1994), pp. 2523–2531.

[13] C. C. Chow and T. Hwa, *Defect mediated stability: An effective hydrodynamic theory of spatiotemporal chaos*, Phys. D, 84 (1995), pp. 494–512.

[14] F. Domínguez-Adame, A. Sánchez, and Yu. S. Kivshar, *Soliton pinning by long range order in aperiodic systems*, Phys. Rev. E, 52 (1995), pp. R2183–R2186.

[15] R. K. Dodd, J. C. Eilbeck, J. D. Gibbon, and H. C. Morris, *Solitons and Nonlinear Waves*, Academic Press, London, 1982.

[16] Z. Fei, V. V. Konotop, M. Peyrard, and L. Vázquez, *Kink dynamics in the periodically modulated ϕ^4 model*, Phys. Rev. E, 48 (1993), pp. 548–554.

[17] Z. Fei and L. Vázquez, *Two energy-conserving numerical schemes for the sine-Gordon equation*, Appl. Math. Comput., 45 (1991), pp. 17–30.

[18] G. Filatrella, B. A. Malomed, and R. D. Parmentier, *Inverse ac Josephson effect for a fluxon in a long modulated junction*, Phys. Lett. A, 198 (1995), pp. 43–50.

[19] G. Filatrella, B. A. Malomed, R. D. Parmentier, and M. Salerno, *Phase locking of fluxons in spatially inhomogeneous Josephson junctions*, Phys. Lett. A, 228 (1997), pp. 250–254.

[20] R. J. Flesch and S. E. Trullinger, *Green's functions for nonlinear Klein-Gordon kink perturbation theory*, J. Math. Phys., 28 (1987), pp. 1619–1631.

[21] M. B. Fogel, S. E. Trullinger, A. R. Bishop, and J. A. Krumhansl, *Classical particlelike behavior of sine-Gordon solitons in scattering potentials and applied fields*, Phys. Rev. Lett. 36 (1976), pp. 1411–1414; M. B. Fogel, S. E. Trullinger, A. R. Bishop, and J. A. Krumhansl, *Dynamics of sine-Gordon solitons in the presence of perturbations*, Phys. Rev. B, 15 (1976), pp. 1578–1592.

[22] A. Galindo and P. Pascual, *Quantum Mechanics I*, Springer-Verlag, Berlin, 1990.

[23] A. A. Golubov, I. L. Serpuchenko, and A. V. Ustinov, *Soliton dynamics in inhomogeneous Josephson junctions: Theory and experiment*, Phys. Lett. A, 130 (1988), pp. 107–110.

[24] S. A. Gredeskul, Yu. S. Kivshar, A. Sánchez, and L. Vázquez, *Kink propagation through disordered media*, Phys. Rev. A, 45 (1992), pp. 8867–8873.

[25] A. Hasegawa, *Optical Solitons in Fibers*, Springer-Verlag, Berlin, 1990.

[26] V. A. Hopkins, J. Keat, G. D. Meegan, T. Zhang, and J. D. Maynard, *Observation of the predicted behavior of nonlinear pulse propagation in disordered media*, Phys. Rev. Lett., 76 (1996), pp. 1102–1105.

[27] S. Jiménez and L. Vázquez, *Analysis of four numerical schemes for a nonlinear Klein-Gordon equation*, Appl. Math. Comput., 35 (1990), pp. 61–94.

[28] D. J. Kaup and A. C. Newell, *Solitons as particles, oscillators, and in slowly changing media: A singular perturbation theory*, Proc. Roy Soc. London Ser. A, 361 (1978), pp. 413–446.

[29] Y. J. Kodama and M. J. Ablowitz, *Perturbations of solitons and solitary waves*, Stud. Appl. Math., 64 (1981), pp. 225–245.

[30] Yu. S. Kivshar, S. A. Gredeskul, A. Sánchez, and L. Vázquez, *Localization decay induced by strong nonlinearity in disordered systems*, Phys. Rev. Lett., 64 (1990), pp. 1693–1696; Yu. S. Kivshar, S. A. Gredeskul, A. Sánchez, and L. Vázquez, *Scattering properties of envelope solitons in disordered systems: Decay of localization effects by strong nonlinearity*, Waves Random Media, 2 (1992), pp. 125–140.

[31] Yu. S. Kivshar and B. A. Malomed, *Dynamics of solitons in nearly integrable systems*, Rev. Modern Phys., 61 (1989), pp. 763–915.

[32] Yu. S. Kivshar and A. Sánchez, *Kink drift in oscillating fields*, Phys. Rev. Lett., 77 (1996), p. 582.

[33] Yu. S. Kivshar, A. Sánchez, O. Chubykalo, A. M. Kosevich, and L. Vázquez, *Interference effects in soliton scattering by impurities*, J. Phys. A, 225 (1992), pp. 5711–5728.

[34] Yu. S. Kivshar, A. Sánchez, and L. Vázquez, *Kink decay in a parametrically driven ϕ^4 chain*, Phys. Rev. A, 45 (1992), pp. 1207–1212.

[35] J. A. Krumhansl and J. R. Schrieffer, *Dynamics and statistical mechanics of a one-dimensional Hamiltonian for structural phase transitions*, Phys. Rev. B, 11 (1975), pp. 3535–3545.
[36] B. A. Malomed and M. I. Tribelsky, *Emission of waves by moving kinks in a spatially modulated sine-Gordon system*, Phys. Rev. B, 41 (1990), pp. 11271–11280.
[37] J. L. Marín, *Intrinsic Localized Modes in Nonlinear Lattices*, Ph.D. thesis, Universidad de Zaragoza, Zaragoza, Spain, 1997; J. L. Marín, S. Aubry, and, L. M. Floria, *Intrinsic localized nodes: Discrete breathers. Existence and linear stability*, Phys. D, 113 (1998), pp. 283–292.
[38] D. W. McLaughlin and A. C. Scott, *Perturbation analysis of fluxon dynamics*, Phys. Rev. A, 18 (1978), pp. 1652–1680.
[39] F. G. Mertens, H. J. Schnitzer, and A. R. Bishop, *Hierarchy of equations of motion for nonlinear coherent excitations applied to magnetic vortices*, Phys. Rev. B, 56 (1997), pp. 2510–2520.
[40] G. S. Mkrtchyan and V. V. Shmidt, *On the radiation from inhomogeneous Josephson junction*, Solid State Commun., 30 (1979), pp. 791–793.
[41] A. C. Newell, *Solitons in Mathematics and Physics*, SIAM, Philadelphia, PA, 1985.
[42] W. I. Newman, D. K. Campbell, and J. M. Hyman, *Identifying coherent structures in nonlinear wave propagation*, Chaos, 1 (1991), pp. 77–94.
[43] P. J. Pascual and L. Vázquez, *Sine-Gordon solitons under weak stochastic perturbations*, Phys. Rev. B, 32 (1985), pp. 8305–8311.
[44] J. K. Perring and T. H. R. Skyrme, *A model unified field equation*, Nuc. Phys., B 31 (1962), pp. 550–555.
[45] M. Peyrard and M. D. Kruskal, *Kink dynamics in the highly discrete sine-Gordon equation*, Phys. D, 14 (1984), pp. 88–102.
[46] W. H. Press, S. A. Teukolsky, *Adaptive stepsize Runge-Kutta integration*, Comp. Phys., 6 (1992), pp. 188–191.
[47] W. H. Press, S. A. Teukolsky, W. T. Vetterling, and B. P. Flannery, *Numerical Recipes in C*, 2nd ed., Cambridge University Press, New York, 1992.
[48] R. Rajaraman, *Solitons and Instantons*, North–Holland, Amsterdam, The Netherlands, 1982.
[49] M. J. Rice and E. J. Mele, *Phenomenological theory of soliton formation in lightly-doped polyacetylene*, Solid State Commun., 35 (1980), pp. 487–491.
[50] M. Rost and J. Krug, *A particle model for the Kuramoto-Sivashinsky equation*, Phys. D, 88 (1995), pp. 1–13.
[51] M. Salerno and Yu. S. Kivshar, *DNA promoters and nonlinear dynamics*, Phys. Lett. A, 193 (1994), pp. 263–266.
[52] A. Sánchez, A. R. Bishop, and F. Domínguez-adame, *Kink stability, propagation, and length-scale competition in the periodically modulated sine-Gordon equation*, Phys. Rev. E, 49 (1994), pp. 4603–4615.
[53] A. Sánchez, R. Scharf, A. R. Bishop, and L. Vázquez, *Sine-Gordon breathers on spatially periodic potentials*, Phys. Rev. A, 45 (1992), pp. 6031–6037.
[54] R. Scharf and A. R. Bishop, *Length-scale competition for the one-dimensional nonlinear Schrödinger equation with spatially periodic potentials*, Phys. Rev. E, 47 (1993), pp. 1375–1383.
[55] R. Scharf and A. R. Bishop, *Soliton chaos in the nonlinear Schrödinger equation with spatially periodic potentials*, Phys. Rev. A, 46 (1992), pp. R2973–R2976.
[56] R. Scharf, Yu. S. Kivshar, A. Sánchez, and A. R. Bishop, *Sine-Gordon kink-antikink generation on spatially periodic potentials*, Phys. Rev. A, 45 (1992), pp. R5369–R5372.
[57] J. Scott-Russell, *Report on waves*, Proc. Roy. Soc. Edinburgh Sect. A (1844), pp. 319-320. See also [15] for an extended quote of the original report. Phys. Rev. B, 28 (1983), pp. 3587–3589.
[58] A. J. Sievers and S. Takeno, *Intrinsic localized modes in anharmonic crystals*, Phys. Rev. Lett., 61 (1988), pp. 970–973.
[59] W. Strauss and L. Vázquez, *Numerical solution of a nonlinear Klein-Gordon equation*, J. Comput. Phys., 28 (1978), pp. 271–278.
[60] A. L. Sukstanskii and K. I. Primak, *Kink drift motion in the ϕ^4 model*, Phys. Rev. Lett., 75 (1995), pp. 3029–3033.
[61] S. Takeno, K. Kisoda, and A. J. Sievers, *Intrinsic localized vibrational modes in anharmonic crystals—stationary modes—*, Prog. Theoret. Phys. Suppl., 94 (1988), pp. 242–269.
[62] E. Tomboulis, *Canonical quantization of nonlinear waves*, Phys. Rev. D, 12 (1975), pp. 1678–1683.
[63] G. B. Whitham, *Linear and Nonlinear Waves*, Wiley, New York, 1974.

[64] C. R. Willis, *Spontaneous emission of a continuum sine-Gordon kink in the presence of a spatially periodic potential*, Phys. Rev. E, 55 (1997), pp. 6097–6100.

[65] C. R. Willis, M. El-Batanouny, and P. Stancioff, *Sine-Gordon kinks on discrete lattices. I. Hamiltonian formalism*, Phys. Rev. B, 33 (1986), pp. 1904-1911; P. Stancioff, C. R. Willis, M. El-Batanouny, and S. Burdick, *Sine-Gordon kinks on discrete lattices.* II. *Static properties*, Phys. Rev. B, 33 (1986), pp. 1912–1920.

[66] N. J. Zabusky, *Computational synergetics and mathematical innovation*, J. Comput. Phys., 43 (1981), pp. 195–249.

[67] N. J. Zabusky and M. D. Kruskal, *Interaction of "solitons" in a collisionless plasma and the recurrence of initial states*, Phys. Rev. Lett., 15 (1965), pp. 240–243.

[68] B. Cano and J. M. Sanz-Serna, *Error growth in the numerical integration of periodic orbits, with application to Hamiltonian and reversible systems*, SIAM J. Numer. Anal., 34 (1997), pp. 1391–1417.

[69] G. Dattoli, P. L. Ottaviani, A. Torre, and L. Vázquez, *Evolution operator equations: Integration with algebraic and finite-difference methods. Applications to physical problems in classical and quantum mechanics and quantum field theory*, Rivista del Nuovo Cimento, 20 (1997), pp. 1–133.

[70] J. de Frutos and J. M. Sanz-Serna, *Accuracy and conservation properties in numerical integration: The case of the Korteweg-de Vries equation*, Numer. Math., 75 (1997), pp. 421–445.

[71] V. V. Konotop and L. Vázquez, *Nonlinear Random Waves*, World Scientific, Singapore, 1994.